Mathematical Biosciences and Engineering

https://www.aimspress.com/journal/mbe

MBE, 23(4): 845–883.
DOI: 10.3934/mbe.2026034
Received: 31 October 2025
Revised: 23 December 2025
Accepted: 05 January 2026
Published: 28 February 2026

Research article

Darwinian dynamics of Host-Pathogen interactions

Anuraag Bukkuri[1,2,*], **Sabrina Streipert**[3] **and Yun Kang**[4]

[1] Department of Mathematics, City St George's, University of London, London, UK
[2] Department of Computational and Systems Biology, University of Pittsburgh, Pittsburgh, USA
[3] Department of Mathematics, University of Pittsburgh, Pittsburgh, USA
[4] Science and Mathematics Faculty, Arizona State University, Mesa, USA

* **Correspondence:** Email: anuraag.bukkuri@city.ac.uk.

Abstract: Epizootic hemorrhagic disease (EHD) causes varied clinical outcomes across ruminants and geographical locations. Northern white-tailed deer experience infrequent, high-mortality outbreaks; southern white-tailed deer experience seasonal, lower-mortality infections; and African cattle experience endemic, subclinical infections. These observations provide a natural setting to explore how environmental exposure impacts the evolution of host defense strategies. In this paper, we develop a Darwinian pathogen-epidemic model that couples host-pathogen population dynamics with the evolution of resistance (recovery from pathogen) and tolerance (minimizing the effects of infection) traits. We obtain the basic reproduction number $\mathcal{R}_0$ and show that the unique disease-free equilibrium is locally asymptotically stable if $\mathcal{R}_0 < 1$ and unstable if $\mathcal{R}_0 > 1$, consistent with the corresponding purely ecological model. However, we also identify key differences between the models, as the evolution of traits can have a stabilizing effect and may promote bistability. Numerical simulations reveal that high pathogen burden and transmission favor the evolution of tolerance, whereas low pathogen burden promotes the evolution of resistance. Host-intrinsic factors, such as natural death rates and density-dependent suppression of growth, lead to resistance evolution, whereas high host reproductive rates lead to tolerance. Applying our model to EHD shows that intermittent exposure in northern deer leads to no evolved defense, seasonal exposure in southern deer results in the evolution of resistance, and endemic exposure in African cattle selects for tolerance. Furthermore, we demonstrate that continuous vs. periodic control of the disease vector population can lead to the evolution of different defense mechanisms. These findings highlight how environmental and host-pathogen factors shape the evolution of defense strategies, thereby informing disease management and control in wildlife and livestock populations affected by pathogens, such as the EHD virus.

Keywords: host-pathogen interactions; Darwinian dynamics; epizootic hemorrhagic disease; eco-evolutionary dynamics; resistance; tolerance; seasonality

1. Introduction

Epizootic hemorrhagic disease (EHD) is caused by the epizootic hemorrhagic disease virus (EHDV), which is transmitted by biting midges [1]. EHD affects a range of ruminant species, from white-tailed deer in North America to cattle in Africa. However, viral loads and clinical symptoms vary greatly across and even within these species due to differences in environmental exposure to EHDV [2]. In the United States, white-tailed deer in northern regions experience sporadic outbreaks of EHD that often lead to high mortality rates. White-tailed deer in southern regions experience seasonal outbreaks of EHD, accompanied by less severe clinical presentation and lower mortality rates than their northern counterparts. African cattle that are exposed to the virus year-round rarely show clinical symptoms despite persistent infection. This variability in disease outcomes across different regions provides a natural framework for understanding how environmental conditions affect host responses to pathogens.

When hosts are confronted with pathogens, the evolution of resistance or tolerance often enables recovery [3,4]. Resistance directly reduces pathogen burden via defense mechanisms, such as immune-mediated viral clearance [5]. Tolerance mechanisms instead aim to minimize the adverse effects of viral infection without directly reducing pathogen load [4] (repairing tissue damage [6] or maintaining reproductive output despite infection [7]). These host defense strategies significantly impact host-parasite dynamics [5, 8, 9] and are associated with physiological costs (due to increased energetic and metabolic demands) that often reduce host reproductive rates [10]. The evolutionary consequences of developing resistance or tolerance are ultimately, of course, dependent on the environmental context.

To investigate how naive hosts evolve defense mechanisms in different environments, we construct a mathematical model grounded in Darwinian dynamics [11, 12]. We begin by formulating an epizoonic system without considering the evolution of host defense mechanisms. Its analysis reveals that the unique disease-free equilibrium is locally asymptotically stable if $\mathcal{R}_0 < 1$ and unstable if $\mathcal{R}_0 > 1$. Interestingly, our analysis shows that the unique endemic equilibrium may lose stability through a Hopf bifurcation. We expand on this model by incorporating the evolution of tolerance and resistance as host defense strategies under a Darwinian dynamics framework. The model explicitly couples the ecological dynamics of susceptible and infected host and pathogen populations with the evolutionary dynamics of resistance and tolerance traits in a structured population modeling framework [13]. A similar analysis reveals a stabilizing effect of the trait evolution with the disappearance of the Hopf bifurcation. It also reveals scenarios of bistability between endemic equilibria, absent in the purely ecological setting. By running numerical simulations of our model, we examine how differences in the environment (e.g., seasonal vs. endemic EHDV exposure), host properties (e.g., reproductive rate, death rate, and density-dependent growth suppression), and pathogen properties (e.g., shedding, transmission, and mortality rates) shape the evolution of defense strategies.

Applying this framework to EHD and considering parameter combinations that represent northern deer, southern deer, and African cattle highlights how environmental context influences the evolution of host defenses. We find that northern deer, experiencing minor and infrequent outbreaks, show limited evolution of resistance or tolerance, reflecting the sporadic nature of selective pressures. Southern deer experience moderate, seasonal outbreaks and evolve resistance, rapidly recovering from viral infections during limited transmission seasons and re-establishing baseline survival levels. Cattle populations under high endemic exposure evolve tolerance, maintaining fitness despite

persistent viral presence rather than attempting to eliminate the pathogen due to the high likelihood of repeated infections. We also show how continuous and periodic control measures on the biting midge vectors can lead to differences in evolved host defense mechanisms. Our work demonstrates how integrating epidemic models with Darwinian dynamics can reveal the evolution of host defense strategies across diverse environmental contexts. Such insights are critical not only for understanding the evolution of host defense systems but also for informing targeted interventions, wildlife management, and disease control strategies in systems affected by pathogens, such as EHDV.

2. Model formulation

2.1. Ecological model

We begin by constructing a classic pathogen-epidemic model that captures the population dynamics of susceptible hosts (S), infected hosts (I), and pathogens in the environment (P):

$$\begin{aligned} \frac{dS}{dt} &= r(S+I)(1-\gamma(S+I)) - \mu S - \beta S P + \phi I \\ \frac{dI}{dt} &= \beta S P - \mu I - \alpha I - \phi I \\ \frac{dP}{dt} &= \omega I - \mu_p P \end{aligned} \tag{2.1}$$

where hosts reproduce to generate susceptible progeny at an intrinsic rate r, constrained by density-dependent factors given by γ. Hosts die at a baseline rate of μ and infected hosts suffer an additional pathogen-induced death rate of α. Susceptible hosts become infected at a rate β and infected individuals recover at a rate ϕ. Pathogens are shed into the environment at a rate ω and decay at a rate μ_p. All model parameters are assumed to be positive, and we consider system (2.1) with nonnegative initial conditions.

Based on the model formulation (2.1), we assume that both the susceptible (S) and infected (I) classes are equally capable of reproduction and possess equal competitive ability for shared resources. Thus, density dependence acts on the total host population $N = S + I$ through the logistic term $rN(1 - \gamma N)$. Furthermore, we assume that infection solely arises from interactions between susceptible individuals (S) and the contaminated environment (P) at a rate $\beta S P$ (there is no direct host-to-host transmission). We also assume that only infected individuals (I) contribute to environmental contamination and that the pathogen (P) is shed into the environment at a rate ωI and decays at a rate $\mu_p P$. We presume that recovery occurs naturally, with infected individuals (I) returning to the susceptible class (S) through their own immune response. This is represented by the recovery term ϕI transitioning from I back to S.

Before incorporating evolutionary dynamics, we analytically explore properties of our purely ecological model (2.1). First, the extinction equilibrium is repellent and therefore unstable for $r > \mu$, which is henceforth assumed.

We can rescale the system by defining

$$n = \gamma N, \qquad x = \frac{S}{N}, \qquad y = \frac{I}{N},$$

where $N = S + I$, so that x, y represent the frequencies of susceptible and infected hosts, respectively.

Clearly $x + y = 1$, and $S = Nx = \frac{n}{\gamma}x$, $I = Ny = \frac{n}{\gamma}y$. Summing the first two equations of (2.1) gives us

$$n' = \gamma N' = n(r(1-n) - \mu - \alpha y).$$

Using $y = I/N$, we have

$$y' = \frac{I'}{N} - y\frac{N'}{N} = \beta x P - (\mu + \alpha + \phi)y - (r(1-n) - \mu - \alpha y)y.$$

Thus,

$$y' = \beta(1-y)P - y\left[r(1-n) + \phi + \alpha(1-y)\right].$$

Since $x = 1 - y$, we obtain immediately $x' = -y'$. Using $I = Ny = \dfrac{n}{\gamma}y$ in the third equation of (2.1), we obtain

$$P' = \frac{\omega n}{\gamma}\, y - \mu_p P.$$

Thus, the rescaled SIP system reads as

$$\begin{aligned} n' &= n\Big(r(1-n) - \mu - \alpha y\Big) \\ y' &= \beta(1-y)P - y\left[r(1-n) + \phi + \alpha(1-y)\right] \\ P' &= \frac{\omega n}{\gamma}\, y - \mu_p P \end{aligned} \tag{2.2}$$

with $x = 1 - y$ and positive parameters.

Theorem 2.1 (Positive invariance, boundedness, and persistence of the rescaled SIP system)**.** *Consider the rescaled SIP system* (2.2)*. Assume*

$$0 < n(0) \le 1, \qquad 0 \le y(0) \le 1, \qquad P(0) \ge 0.$$

Then, the following hold:

i) $n(t), y(t), P(t) \ge 0$ *for all* $t \ge 0$.
ii) $n(t) \le 1$ *for all* $t \ge 0$.
iii) $y(t) < 1$ *for all* $t > 0$.
iv) $P(t)$ *is uniformly bounded for* $t \ge 0$.
v) If additionally $r > \mu + \alpha$*, then* n *is persistent away from zero (there exists* $\delta > 0$ *such that* $\liminf_{t\to\infty} n(t) \ge \delta > 0$*).*

Proof. Since the right-hand side of (2.2) is a polynomial in (n, y, P), local existence and uniqueness follow from standard ODE theory.

To prove i), we show that $n(t) \ge 0$ for all $t \ge 0$. Since

$$\frac{dn}{dt} = n\Big(r(1-n) - \mu - \alpha y\Big),$$

we have at any point where $n = 0$, $\frac{dn}{dt}\Big|_{n=0} = 0$. Thus, the hyperplane $n = 0$ is invariant. Since $n(0) > 0$, it follows that $n(t) \geq 0$ for all $t \geq 0$.

We prove positivity of y and P simultaneously by a first-exit argument. Define

$$t^* := \inf\{t > 0 : \ y(t) < 0 \text{ or } P(t) < 0\}.$$

Suppose for contradiction that $t^* < \infty$. By continuity, for all $0 \leq t < t^*$, we have $y(t) \geq 0$ and $P(t) \geq 0$, and at $t = t^*$ at least one of y, P equals zero while the other is still nonnegative. We now examine the vector field on the boundary sets $y = 0$ and $P = 0$, recalling that $n(t) \geq 0$ for all $t \geq 0$.

Case 1: $y(t^*) = 0$ *and* $P(t^*) \geq 0$. From (2.2),

$$\frac{dy}{dt}\Big|_{y=0} = \beta(1-0)P - (\alpha+\phi)0 - r\cdot 0\cdot(1-n) + \alpha\cdot 0^2 = \beta P \ \geq \ 0.$$

Hence, the vector field at $y = 0$ points into the region $y \geq 0$, so y cannot decrease through zero.

Case 2: $P(t^*) = 0$ *and* $y(t^*) \geq 0$. Again from (2.2),

$$\frac{dP}{dt}\Big|_{P=0} = \frac{\omega n}{\gamma} y \ \geq \ 0$$

since $n \geq 0$ and $y \geq 0$ for $t \leq t^*$. Thus, the vector field at $P = 0$ also points into the region $P \geq 0$ and P cannot decrease through zero. In either case, we obtain a contradiction with the definition of t^*. Therefore, $t^* = \infty$ and $y(t), P(t) \geq 0$, for all $t \geq 0$.

To prove ii), we now show that the interval $[0, 1]$ is invariant for n. By i), $n(t) \geq 0$ for all $t \geq 0$. At $n = 1$, the equation for n gives

$$\frac{dn}{dt}\Big|_{n=1} = 1\cdot\big(r(1-1) - \mu - \alpha y\big) = -\mu - \alpha y \ \leq \ -\mu \ < 0.$$

Thus, on the boundary $n = 1$, the vector field points strictly towards the region $n < 1$. By the standard invariance theorem for ODEs, if $n(0) \leq 1$ then $0 \leq n(t) \leq 1$ for all $t \geq 0$.

We next show iii), that is, y remains in the interval $[0, 1]$ and, for $t > 0$, actually lies in $(0, 1]$ (given $y(0) \leq 1$). Recall $y \geq 0$ for $t \geq 0$ from i). Evaluate the equation for y at $y = 1$:

$$\frac{dy}{dt}\Big|_{y=1} = \beta(1-1)P - (\alpha+\phi)\cdot 1 - r\cdot 1\cdot(1-n) + \alpha\cdot 1^2 = -\phi - r(1-n) < 0,$$

since $n \leq 1$, by ii). Thus, on the boundary $y = 1$, the vector field points strictly towards the region $y < 1$, completing the claim.

To show iv), we recall that $0 \leq n(t) \leq 1$ and $0 \leq y(t) < 1$ for all $t \geq 0$. Hence,

$$\frac{dP}{dt} = \frac{\omega n}{\gamma} y - \mu_p P \leq \frac{\omega}{\gamma} - \mu_p P.$$

Since the solution to the linear equation $\frac{dQ}{dt} = \frac{\omega}{\gamma} - \mu_p Q$, with the same initial conditions $Q(0) = P(0)$, converges monotonically to its equilibrium $Q^* = \dfrac{\omega}{\gamma\mu_p}$, we have, by a comparison argument that

$$0 \leq P(t) \leq Q(t) \leq \max\left\{P(0), \frac{\omega}{\gamma\mu_p}\right\}, \qquad \text{for all } t \geq 0.$$

Thus, $P(t)$ is uniformly bounded.

Lastly, we show v). Since $0 \le y(t) < 1$ for all $t > 0$, we have

$$\frac{dn}{dt} = n\Big(r(1-n) - \mu - \alpha y\Big) \ge n\Big(r(1-n) - \mu - \alpha \cdot 1\Big) = n\Big((r-\mu-\alpha) - rn\Big).$$

Define $L := \dfrac{r-\mu-\alpha}{r}$, then, by assumption, $L > 0$. Again, we utilize a comparison argument. We consider the logistic differential equation

$$\frac{dm}{dt} = m((r-\mu-\alpha) - rm), \qquad m(0) = n(0) > 0.$$

Its unique equilibrium in $(0,1)$ is $m = L$, and $m(t) \to L$ as $t \to \infty$. Since, $\frac{dn}{dt} \ge \frac{dm}{dt}$ whenever $n(t) = m(t)$, the comparison theorem yields $n(t) \ge m(t)$ for all $t \ge 0$.

Taking lim inf as $t \to \infty$,

$$\liminf_{t\to\infty} n(t) \ \ge \ \lim_{t\to\infty} m(t) = L = \frac{r-\mu-\alpha}{r} =: \delta > 0.$$

Thus n is persistent away from zero. □

The theorem of positive invariant and boundedness for the rescales system (2.2) is equivalent to showing that the original system (2.1) is positive and invariant in the bounded space of $N(t) = S(t) + I(t) \le \frac{1}{\gamma}$, the fact that suplim of $y(t) < 1$ shows that $S(t)$ is bounded above zero (persistent).

If $r > \mu$, then there exists a unique disease-free equilibrium (DFE), where $I = P = 0$ and $S > 0$ satisfies

$$0 = rS(1-\gamma S) - \mu S = S[r(1-\gamma S) - \mu].$$

Thus, the unique DFE is given by

$$E_0 = (S_0, 0, 0) = \left(\frac{r-\mu}{r\gamma},\ 0,\ 0\right).$$

We define the basic reproduction number as

$$\mathcal{R}_0 := \frac{\beta\omega S_0}{\mu_p(\mu+\alpha+\phi)} = \frac{\beta\omega}{\mu_p(\mu+\alpha+\phi)} \cdot \frac{(r-\mu)}{r\gamma}. \tag{2.3}$$

Theorem 2.2. *Consider* (2.1) *and* $\mathcal{R}_0$ *given in* (2.3). *If* $\mathcal{R}_0 < 1$, *then* E_0 *is locally asymptotically stable. If* $\mathcal{R}_0 > 1$, *then* E_0 *is a saddle and, therefore, unstable.*

Proof. The Jacobian evaluated at E_0 is given by

$$J(E_0) = \begin{bmatrix} -(r-\mu) & \phi - (r-2\mu) & -\frac{\beta}{\gamma}(1-\frac{\mu}{r}) \\ 0 & -\alpha-\mu-\phi & \frac{\beta}{\gamma}(1-\frac{\mu}{r}) \\ 0 & \omega & -\mu_p \end{bmatrix}$$

with eigenvalue $-(r-\mu)$ and the solutions to

$$\lambda^2 + (\mu+\alpha+\mu_p+\phi)\lambda + (\mu+\alpha+\phi)\mu_p - \frac{\beta\omega}{\gamma}\left(1-\frac{\mu}{r}\right) = 0.$$

By Descartes' rule of signs, there exists a unique positive solution if

$$(\mu+\alpha+\phi)\mu_p < \frac{\beta\omega}{\gamma}\left(1-\frac{\mu}{r}\right) \qquad \Longleftrightarrow \qquad \mathcal{R}_0 > 1.$$

Instead, if the inequality is reversed, then both solutions have negative real parts. This completes the claim. □

We continue our analysis by discussing the existence of an endemic equilibrium E^*. This is an equilibrium of the form $E^* = (S^*, I^*, P^*)$, where all components are positive.

Theorem 2.3. *Consider* (2.1) *with* $\mathcal{R}_0$ *given in* (2.3). *If* $\mathcal{R}_0 > 1$, *then there exists a unique endemic equilibrium given by* $E^* = (S^*, I^*, P^*)$, *where*

$$S^* = \frac{\mu_p(\mu+\alpha+\phi)}{\beta\omega}, \qquad I^* = N^* - S^*, \qquad P^* = \frac{\omega}{\mu_p}I^*,$$

where

$$N^* = \frac{(r-\mu-\alpha) + \sqrt{(r-\mu-\alpha)^2 + 4r\gamma\alpha S^*}}{2r\gamma}. \tag{2.4}$$

If $\mathcal{R}_0 \leq 1$, *then there exists no endemic equilibrium.*

Proof. By the last equation of (2.1), $P^* = \dfrac{\omega}{\mu_p}I^*$. Substituting this into the second equation of (2.1) gives

$$\beta S^*\left(\frac{\omega}{\mu_p}I^*\right) = (\mu+\alpha+\phi)I^*$$

so that for $I^* > 0$, the endemic susceptible level satisfies

$$S^* = \frac{\mu_p(\mu+\alpha+\phi)}{\beta\omega}, \tag{2.5}$$

which is positive for all $\beta, \omega, \mu_p, \mu, \alpha, \phi > 0$ and is independent of r and γ. Adding the first two equations in (2.1) gives the dynamics of the total host population $N = S + I$. At equilibrium,

$$0 = rN^*(1-\gamma N^*) - \mu S^* - (\mu+\alpha)I^*.$$

Substituting $I^* = N^* - S^*$ yields

$$P(N^*) := r\gamma(N^*)^2 + (\mu+\alpha-r)N^* - \alpha S^* = 0, \tag{2.6}$$

which has exactly one positive root given by (2.4). Then, the endemic components I^* and P^* are explicitly given by the relations

$$I^* = N^* - S^*, \qquad P^* = \frac{\omega}{\mu_p}I^*.$$

Since N^* is the only positive root and the leading coefficient of $P(u)$ is positive, we know that $P(u) < 0$ for all $0 < u < N^*$ and $P(u) > 0$ for all $u > N^*$. Utilizing this and noticing that

$$P(S^*) = \frac{\mu_p}{\beta^2\omega^2}(\alpha+\mu+\phi)\gamma\mu_p(\alpha+\mu+\phi)r - \beta\omega(r-\mu)$$

$$= \frac{\mu_p}{\beta^2\omega^2}(\alpha+\mu+\phi)\gamma\mu_p(\alpha+\mu+\phi)r(1-\mathcal{R}_0) < 0$$

for $\mathcal{R}_0 > 1$, we can conclude that $N^* > S^*$ and, therefore, $I^*, P^* > 0$. Thus, if $\mathcal{R}_0 > 1$, then there exists a unique endemic equilibrium. If $\mathcal{R}_0 \leq 1$, then there exists no endemic equilibrium. □

Theorem 2.4. *Consider* (2.1) *with* $\mathcal{R}_0$ *given in* (2.3). *If* $\mathcal{R}_0 > 1$ *and* $Q_1(N^*) := b_0 + b_1N^* > 0$ *and* $Q_2(N^*) := (c_0 + c_1N^*)(b_0 + b_1N^*) - (d_0 + d_1N^* + d_2(N^*)^2) > 0$, *where*

$$b_1 = \beta\omega - \frac{\beta\omega}{\mu_p}(\mu+\alpha-r) + 2\mu_p\gamma r, \qquad b_0 = 2\alpha(\alpha+\mu+\phi) - (\alpha+\mu_p)(\alpha+\phi) - \alpha\mu - r\mu_p,$$

$$c_1 = \frac{\beta\omega}{\mu_p} + 2\gamma r, \qquad c_0 = \mu + \mu_p - r, \qquad d_2 = 2\beta\omega\gamma r, \qquad d_1 = \beta\omega(\alpha+\mu-r(1+2\gamma S^*)), \qquad d_0 = -\beta\omega(\alpha+\mu-r)S^*,$$

N^* *is given in* (2.4), *and* S^* *is given in* (2.5), *then the unique endemic equilibrium* E^* *given in Theorem 2.3 is locally asymptotically stable. If* $\min\{Q_1(N^*), Q_2(N^*)\} < 0$, *then* E^* *is unstable.*

Proof. For $\mathcal{R}_0 > 1$, the Jacobian at E^* is

$$J(N^*, S^*, P^*) = \begin{bmatrix} -\beta P^* - \mu + r(1-2\gamma N^*) & \phi + r(1-2\gamma N^*) & -\beta S^* \\ \beta P^* & -(\alpha+\mu+\phi) & \beta S^* \\ 0 & \omega & -\mu_p \end{bmatrix}$$

so that, after expanding around the last row, and introducing $k = r(1-2\gamma N^*)$,

$$\begin{aligned}
\det(J-\lambda I) &= -\omega\beta S^*\left[r(1-2\gamma N^*) - \lambda - \mu\right] + (-\lambda-\mu_p)\left\{\beta P^*[\lambda+\mu+\alpha-r(1-2\gamma N^*)]\right. \\
&\qquad \left. + (\lambda+\alpha+\mu+\phi)\left[\lambda+\mu-r(1-2\gamma N^*)\right]\right\} \\
&= \mu_p(\mu+\alpha+\phi)\left[\lambda+\mu-k\right] + (-\lambda-\mu_p)\left[\beta\frac{\omega}{\mu_p}I^*(\lambda+\mu+\alpha-k) + (\lambda+\alpha+\mu+\phi)\left[\lambda+\mu-k\right]\right] \\
&= -\beta\frac{\omega}{\mu_p}I^*(\lambda+\mu_p)(\lambda+\mu+\alpha-k) + \left[\lambda+\mu-k\right]\left[\mu_p(\mu+\alpha+\phi) - (\lambda+\mu_p)(\lambda+\alpha+\mu+\phi)\right] \\
&= -\beta\frac{\omega}{\mu_p}I^*(\lambda+\mu_p)(\lambda+\mu-k+\alpha) - \lambda(\lambda+\mu-k)(\lambda+\alpha+\mu+\phi+\mu_p) \\
&= (\lambda+\mu-k+\alpha)\left[-\beta\frac{\omega}{\mu_p}I^*(\lambda+\mu_p) - \lambda(\lambda+\alpha+\mu+\phi+\mu_p)\right] + \alpha\lambda(\lambda+\alpha+\mu+\phi+\mu_p) \\
&= (\lambda+\mu-k+\alpha)\left[-\lambda^2 - \left(\beta\frac{\omega N^*}{\mu_p} + \mu_p\right)\lambda + \mu_p(\alpha+\mu+\phi) - \beta\omega N^*\right] + \alpha\lambda(\lambda+\alpha+\mu+\phi+\mu_p) \\
&= -(\lambda^3 + a_2\lambda^2 + a_1\lambda + a_0),
\end{aligned}$$

where

$$\begin{aligned}
a_0 &= \beta\omega(\alpha-k+\mu)\left(N^* - \frac{\mu_p(\alpha+\mu+\phi)}{\beta\omega}\right) = \beta\omega(\alpha-k+\mu)(N^*-S^*) = d_0 + d_1N^* + d_2(N^*)^2, \\
a_1 &= \frac{N^*\beta\omega}{\mu_p}(\alpha-k+\mu+\mu_p) - (\alpha+\mu_p)(\alpha+\phi) - \alpha\mu - k\mu_p, \\
a_2 &= \frac{N^*\beta\omega}{\mu_p} - k + \mu + \mu_p = c_0 + c_1N^*.
\end{aligned}$$

The Routh-Hurwitz conditions, to guarantee the local asymptotic stability of E^*, are

$$a_0, a_1, a_2 > 0 \qquad \text{and} \quad a_2 a_1 > a_0.$$

First, we show that $a_0 > 0$ by proving that $\alpha + \mu > k$. Since

$$N^* = \frac{r - \mu - \alpha + \sqrt{(r-\mu-\alpha)^2 + 4r\gamma\alpha S^*}}{2r\gamma} > \frac{r-\mu-\alpha}{2r\gamma},$$

which is, after rearranging, equivalent to $\alpha + \mu > r\,(1 - 2\gamma N^*) = k$. Thus, $a_0 > 0$. To show that $a_2 > 0$, we first note that

$$N^* > S^* \quad \Longleftrightarrow \quad N^* > \frac{\mu_p(\alpha+\mu+\phi)}{\beta\omega} \quad \Longleftrightarrow \quad \frac{N^*\beta\omega}{\mu_p} > \alpha + \mu + \phi.$$

Thus,

$$a_2 = \frac{N^*\beta\omega}{\mu_p} + \mu + \mu_p - k > \alpha + \mu + \phi + \mu + \mu_p - k > \alpha + \mu - k > 0,$$

where the last inequality follows from the calculations that $a_0 > 0$.

To investigate the sign of a_1, we recall that N^* solves $P(N^*) = 0$, where P is given in (2.6). Then, using that $k = r(1 - 2\gamma N^*)$, we get

$$\begin{aligned}
a_1 &= \frac{N^*\beta\omega}{\mu_p}(\alpha - k + \mu + \mu_p) - (\alpha+\mu_p)(\alpha+\phi) - \alpha\mu - k\mu_p \\
&= \frac{N^*\beta\omega}{\mu_p}(\alpha + \mu + \mu_p - r) + 2\gamma\frac{(N^*)^2\beta\omega}{\mu_p} - (\alpha+\mu_p)(\alpha+\phi) - \alpha\mu - r\mu_p + 2\mu_p\gamma r N^* \\
&= \frac{N^*\beta\omega}{\mu_p}(\alpha + \mu + \mu_p - r) + 2\frac{\beta\omega}{\mu_p}(\alpha S^* - (\mu + \alpha - r)N^*) - (\alpha+\mu_p)(\alpha+\phi) - \alpha\mu - r\mu_p + 2\mu_p\gamma r N^* \\
&= N^*\left\{\beta\omega - \frac{\beta\omega}{\mu_p}(\mu + \alpha - r) + 2\mu_p\gamma r\right\} + 2\alpha(\alpha+\mu+\phi) - (\alpha+\mu_p)(\alpha+\phi) - \alpha\mu - r\mu_p \\
&= b_1 N^* + b_0 =: Q_1(N^*)
\end{aligned}$$

The rest follows from the Routh-Hurwitz conditions. □

Numerical simulations for the parameters $r = 0.2383286$, $\gamma = 0.1$, $\mu = 0.09265338$, $\phi = 0.0852610$, $\alpha = 1.0468965$, $\omega = 2$, and $\mu_p = 1.0379858$ suggest the existence of a Hopf bifurcation for increasing values of β, see Figure 1. Since $\mathcal{R}_0$ is proportional to the transmission rate β, it suggests that the system first undergoes a transcritical bifurcation at $\mathcal{R}_0$ but with further increasing $\mathcal{R}_0$ undergoes a Hopf bifurcation, giving rise to an attracting limit cycle. The loss of stability of the endemic equilibrium through a Hopf bifurcation is consistent with earlier work that demonstrates that in systems where epidemiological and demographic processes are coupled, especially those with high pathogenicity or latent periods, the system often settles into stable limit cycles rather than a fixed equilibrium [14].

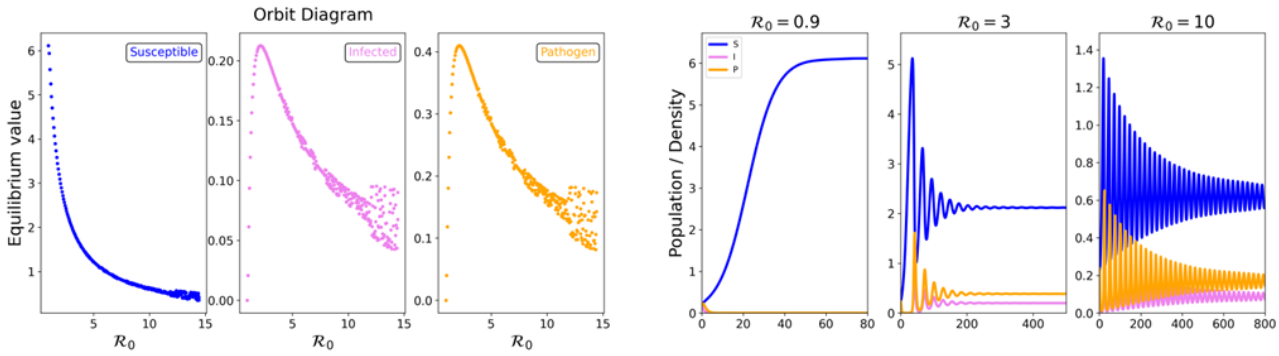

Figure 1. Left: Orbit diagram, showing the minimum and maximum values after run-in period of 1 million for the variables S, I, P for varying β expressed as dependency on $\mathcal{R}_0 \propto \beta$. Right: Dynamics of the variables S, I, P for different values of $\mathcal{R}_0$, highlighting the transition from the convergence to the DFE, to the unique endemic equilibrium, and with further increase of $\mathcal{R}_0$, the convergence to a limit cycle.

2.2. Eco-evolutionary model

To incorporate evolutionary dynamics into this system, we turn to Darwinian dynamics. This formalism, rooted in evolutionary game theory, was originally developed to describe interactions among species while accounting for their phenotypic traits (or strategies) [11, 12]. Since then, it has been used to explain the evolution of the traits of harvested populations [15], changes in age distribution [13, 16], and has been applied to develop novel evolutionarily-informed therapies for cancer [17–21]. However, its application to epidemic systems remains scarce (for an exception, see [22]).

To transform our basic epizootic model into a Darwinian dynamics model, we first choose the relevant evolutionary strategies. Since we are interested in host defense strategies against pathogen infection, we introduce two strategies: v_r, representing resistance, and v_t, capturing tolerance. Resistance allows hosts to mount a stronger immunological response (e.g., a faster and stronger type I interferon response), thereby accelerating recovery from infection. Accordingly, we model the recovery rate ϕ as an increasing function of v_r. In contrast, tolerance allows hosts to coexist with the pathogenic infection (e.g., by promoting tissue resilience), thereby reducing their disease-induced death rate. Thus, we let the disease-induced death rate α decrease as a function of v_t. In addition, to account for the life history trade-offs that accompany the development of resistance and tolerance defense mechanisms [10], we include a cost in the intrinsic growth rate by letting r be a decreasing function of v_r and v_t. Thus, our updated ecological model is given by:

$$\begin{aligned}
\frac{dS}{dt} &= r(v_r, v_t)(S + I)(1 - \gamma(S + I)) - \mu S - \beta S P + \phi(v_r) I \\
\frac{dI}{dt} &= \beta S P - \mu I - \alpha(v_t) I - \phi(v_r) I \\
\frac{dP}{dt} &= \omega I - \mu_p P,
\end{aligned} \tag{2.7}$$

where

$$r(v_r, v_t) = \overline{r}e^{-\frac{v_r^2+v_t^2}{\sigma_r^2}}, \qquad \alpha(v_t) = \overline{\alpha}e^{-\frac{v_t^2}{\sigma_\alpha^2}}, \qquad \phi(v_r) = \overline{\phi}\left(1 - e^{-\frac{v_r^2}{\sigma_\phi^2}}\right).$$

We use an exponential decay functional form that asymptotes to 0 for r and α as we assume that evolving resistance or tolerance decreases the disease-induced death rate and the reproductive rate of the host. In the extreme case, when the organism allocates all of its efforts into defending against the disease, we presume that both disease-induced death and reproduction approach 0. Similarly, we use a $1 - \exp(-x)$ functional form for ϕ, assuming that evolving resistance and tolerance can increase the recovery rate, but only up to a biophysical threshold. The assumption that these values only vary with v_r and v_t is a model simplification–in reality, these parameters may also change in response to environmental or pathogenic properties. The equations determining how v_r and v_t evolve are given by Darwinian dynamics. A crucial assumption in this modeling framework is that the traits v_i evolve towards increased fitness. In general, this is described by $v_i' = k\frac{\partial G}{\partial v_i}$, where G captures the fitness. For state-structured models, the fitness is described by the spectral bound of the population projection matrix A that captures transitions among susceptible and resistant hosts [13, 21, 23–25]: $G = \rho(A) = \max\{\Re(\lambda) : \lambda \in \sigma(\mathbf{A})\} = \lim_{t\to\infty} \frac{1}{t}\log\|e^{t\mathbf{A}}\|$ where $e^{t\mathbf{A}} = \sum_{k=0}^{\infty} t^k\mathbf{A}^k/k!$ is the matrix exponential, $\sigma(A)$ is the spectrum of $\mathbf{A}$, and $\Re(\lambda)$ denotes the real part of λ. We can perform a spectral decomposition to represent the number of susceptible and infected hosts as $\mathbf{n}(t) = \sum_i c_i e^{\lambda_i t}\mathbf{w}_i$ where λ_i is the ith eigenvalue of $\mathbf{A}$, c_i is a constant chosen such that $\mathbf{n}(t) = \sum_i c_i\mathbf{w_i}$, and $\mathbf{w}_i$ is its corresponding right eigenvector. As $t \to \infty$, this quantity is dominated by $\rho(A)$ as the contributions from the other eigenvalues disappear over time, and the demographic structure (i.e., proportion of susceptible and infected hosts) converges to $\mathbf{w}_i$: $\mathbf{n}(t \to \infty) \approx c_b e^{\lambda_b t}\mathbf{w}_b$. This fitness metric, which is evaluated at each time step in our simulations, thus captures the asymptotic, long-term growth rate of the host population under the existing ecological and environmental conditions. Although it may initially seem appealing to instead use the total host population size as a proxy for fitness, this may lead to inaccurate evolutionary trajectories since it inherently assumes uniform stage-specific reproductive values. In other words, it assumes that infected and susceptible individuals contribute equally to the fitness of the host population. However, this assumption does not hold whenever the pathogen exists in the environment due to the non-zero disease-induced mortality in the infected component.

Thus, our evolutionary dynamics are given by:

$$\frac{dv_i}{dt} = k\left(\frac{\partial}{\partial v_i}\rho(A(v_r, v_t)\right),$$

where $A = A(v_r, v_t) = A(S, I, P, v_r, v_t)$ is the projection matrix describing the movement between the classes S and I and k captures evolvability. For (2.7), we have

$$A(v_r, v_t) = \begin{bmatrix} r(v_r, v_t)\,(1 - \gamma(S + I)) - \mu - \beta P & r(v_r, v_t)\,(1 - \gamma(S + I)) + \phi(v_r) \\ \beta P & -\mu - \alpha(v_t) - \phi(v_r) \end{bmatrix}. \tag{2.8}$$

We therefore propose the following Darwinian epizootic tolerance model:

$$\begin{aligned}\frac{dS}{dt} &= r(v_r, v_t)(S+I)\,(1-\gamma(S+I)) - \mu S - \beta S P + \phi(v_r) I\\ \frac{dI}{dt} &= \beta S P - \mu I - \alpha(v_t) I - \phi(v_r) I\\ \frac{dP}{dt} &= \omega I - \mu_p P\\ \frac{dv_i}{dt} &= k\left(\frac{\partial}{\partial v_i}\rho(A(v_r, v_t))\right),\end{aligned} \tag{2.9}$$

where $A\colon \mathbb{R}_0^+ \times \mathbb{R}_0^+ \to \mathbb{R}\times\mathbb{R}$ is given in (2.8) and all model parameters are positive.

We require and henceforth assume that $\bar{r} > \mu$–otherwise, the population goes extinct even in the absence of the disease and despite the largest reproductive strength. Since the parameters v_r, v_t only result in varying parameters r, ϕ, α all of which remain positive independent of the precise values of v_r, v_t and using that $r(v_r, v_t) \le \bar{r}, \alpha(v_t) \le \overline{\alpha}$, and $\phi(v_r) \le \overline{\phi}$, we can exploit a similar argument as in Theorem 2.1 to prove that S, I, P remain nonnegative and bounded.

To further analyze (2.9), we obtain the disease-free equilibria (DFE). These are equilibria of the form $E_0 = (S^*, I^*, P^*, v_r^*, v_t^*)$ with $I^* = 0 = P^*$ and $S^* > 0$. Furthermore, S^*, v_r^*, v_t^* must satisfy

$$0 = r(v_r^*, v_t^*)S^*(1-\gamma S^*) - \mu S^* \qquad \text{and} \qquad 0 = \frac{\partial}{\partial v_i}\rho(A(v_r^*, v_t^*)), \qquad i \in \{r, t\}.$$

The first equation implies that

$$S^* = \frac{1}{\gamma}\left(1 - \frac{\mu}{r(v_r^*, v_t^*)}\right).$$

To determine v_i^* for $i \in \{r, t\}$, we note that the spectral bound of A is

$$\rho(A) = \begin{cases} \frac{\mathrm{tr}(A) \pm \sqrt{(\mathrm{tr}(A))^2 - 4\det(A)}}{2} & \text{if } \mathrm{tr}(A)^2 - 4\det(A) > 0\\ \frac{\mathrm{tr}(A)}{2} & \text{if } \mathrm{tr}(A)^2 - 4\det(A) \le 0 \end{cases} \tag{2.10}$$

where

$$\mathrm{tr}(A) = r(v_r, v_t)\,(1-\gamma(S+I)) - \mu - \beta P - \mu - \alpha(v_t) - \phi(v_r)$$

and

$$\begin{aligned}\det(A) &= (r(v_r, v_t)\,(1-\gamma(S+I)) - \mu - \beta P)\,(-\mu - \alpha(v_t) - \phi(v_r)) - (r(v_r, v_t)\,(1-\gamma(S+I)) + \phi(v_r))\beta P\\ &= -r(v_r, v_t)\,(1-\gamma(S+I))\,(\mu + \alpha(v_t) + \phi(v_r) + \beta P) + \mu(\mu + \alpha(v_t) + \phi(v_r)) + \beta P(\mu + \alpha(v_t)).\end{aligned}$$

Since

$$\begin{aligned}&\left\{\mathrm{tr}(A)^2 - 4\det(A)\right\}\Big|_{S=S^*, I=P=0}\\ &\quad= (-\mu - \alpha(v_t) - \phi(v_r))^2 - 4\,(-\mu\,(\mu + \alpha(v_t) + \phi(v_r)) + \mu(\mu + \alpha(v_t) + \phi(v_r)))\\ &\quad= (\mu + \alpha(v_t) + \phi(v_r))^2 > 0,\end{aligned}$$

we have, recalling (2.10),

$$\frac{\partial}{\partial v_i}\rho(A)\Big|_{S=S^*,I=P=0} = \frac{\partial}{\partial v_i}\frac{\mathrm{tr}(A) + \sqrt{(\mathrm{tr}(A))^2 - 4\det(A)}}{2}\Big|_{S=S^*,I=P=0}.$$

Thus, v_i^*, for $i \in \{r, t\}$, are obtained by solving

$$0 = \frac{\partial\rho(A)}{\partial v_i}\Big|_{S=S^*,I=P=0} = \frac{1}{2}\frac{\partial \mathrm{tr}(A)}{\partial v_i} + \frac{\mathrm{tr}(A)\left(\frac{\partial}{\partial v_i}\mathrm{tr}(A)\right) - 2\left(\frac{\partial}{\partial v_i}\det(A)\right)}{2\sqrt{(\mathrm{tr}(A))^2 - 4\det(A)}}\Big|_{S=S^*,I=P=0}.$$

Evaluating the partial derivatives (see details in Appendix) at $S = S^*$ and $I = 0 = P$, we get

$$\begin{aligned}
\frac{\partial \mathrm{tr}(A)}{\partial v_r}\Big|_{S=S^*,I=P=0} &= \frac{-2v_r}{\sigma_r^2}\mu - \frac{2v_r}{\sigma_\phi^2}\overline{\phi}e^{-\frac{v_r^2}{\sigma_\phi^2}} = -2v_r\left\{\frac{\mu}{\sigma_r^2} + \frac{\overline{\phi}}{\sigma_\phi^2}e^{-\frac{v_r^2}{\sigma_\phi^2}}\right\},\\
\frac{\partial \mathrm{tr}(A)}{\partial v_t}\Big|_{S=S^*,I=P=0} &= \frac{-2v_t}{\sigma_r^2}\mu + \frac{2v_t}{\sigma_\alpha^2}\alpha(v_t) = -2v_t\left\{\frac{\mu}{\sigma_r^2} - \frac{\alpha(v_t)}{\sigma_\alpha^2}\right\},\\
\frac{\partial \det(A)}{\partial v_r}\Big|_{S=S^*,I=P=0} &= \frac{2v_r}{\sigma_r^2}\mu\left(\mu + \alpha(v_t) + \phi(v_r)\right),\\
\frac{\partial \det(A)}{\partial v_t}\Big|_{S=S^*,I=P=0} &= \frac{2v_t}{\sigma_r^2}\mu\left(\mu + \alpha(v_t) + \phi(v_r)\right).
\end{aligned}$$

Thus,

$$\begin{aligned}
\frac{\partial}{\partial v_r}\sqrt{(\mathrm{tr}(A))^2 - 4\det(A)}\Big|_{S=S^*,I=P=0} &= \frac{2\mathrm{tr}(A)\left(\frac{\partial}{\partial v_r}\mathrm{tr}(A)\right) - 4\left(\frac{\partial}{\partial v_r}\det(A)\right)}{2\sqrt{(\mathrm{tr}(A))^2 - 4\det(A)}}\Big|_{S=S^*,I=P=0}\\
&= \frac{-4(-\mu - \alpha(v_t) - \phi(v_r))v_r\left\{\frac{\mu}{\sigma_r^2} + \frac{\overline{\phi}e^{-\frac{v_r^2}{\sigma_\phi^2}}}{\sigma_\phi^2}\right\} - 8\frac{v_r}{\sigma_r^2}\mu\left(\mu + \alpha(v_t) + \phi(v_r)\right)}{2(\mu + \alpha(v_t) + \phi(v_r))}\\
&= 2v_r\left\{\frac{\overline{\phi}e^{-\frac{v_r^2}{\sigma_\phi^2}}}{\sigma_\phi^2} - \frac{\mu}{\sigma_r^2}\right\}
\end{aligned}$$

and

$$\begin{aligned}
\frac{\partial}{\partial v_t}\sqrt{(\mathrm{tr}(A))^2 - 4\det(A)}\Big|_{S=S^*,I=P=0} &= \frac{2\mathrm{tr}(A)\left(\frac{\partial}{\partial v_t}\mathrm{tr}(A)\right) - 4\left(\frac{\partial}{\partial v_t}\det(A)\right)}{2\sqrt{(\mathrm{tr}(A))^2 - 4\det(A)}}\Big|_{S=S^*,I=P=0}\\
&= \frac{-4(-\mu - \alpha(v_t) - \phi(v_r))v_t\left\{\frac{\mu}{\sigma_r^2} - \frac{\alpha(v_t)}{\sigma_\alpha^2}\right\} - 8\frac{v_t}{\sigma_r^2}\mu\left(\mu + \alpha(v_t) + \phi(v_r)\right)}{2(\mu + \alpha(v_t) + \phi(v_r))}\\
&= -2v_t\left\{\frac{\alpha(v_t)}{\sigma_\alpha^2} + \frac{\mu}{\sigma_r^2}\right\}.
\end{aligned}$$

Hence,

$$\frac{\partial\rho(A)}{\partial v_r}\Big|_{S=S^*,I=P=0} = \frac{1}{2}\frac{\partial \mathrm{tr}(A)}{\partial v_r} + \frac{1}{2}\frac{\partial}{\partial v_r}\sqrt{(\mathrm{tr}(A))^2 - 4\mathrm{det}(A)}\Big|_{S=S^*,I=P=0}$$
$$= -v_r\left\{\frac{\mu}{\sigma_r^2} + \frac{\overline{\phi}}{\sigma_\phi^2}e^{-\frac{v_r^2}{\sigma_\phi^2}}\right\} + v_r\left\{\frac{\overline{\phi}e^{-\frac{v_r^2}{\sigma_\phi^2}}}{\sigma_\phi^2} - \frac{\mu}{\sigma_r^2}\right\} = -2v_r\frac{\mu}{\sigma_r^2}$$

and

$$\frac{\partial\rho(A)}{\partial v_t}\Big|_{S=S^*,I=P=0} = \frac{1}{2}\frac{\partial \mathrm{tr}(A)}{\partial v_t} + \frac{1}{2}\frac{\partial}{\partial v_t}\sqrt{(\mathrm{tr}(A))^2 - 4\mathrm{det}(A)}\Big|_{S=S^*,I=P=0}$$
$$= -v_t\left\{\frac{\mu}{\sigma_r^2} - \frac{\alpha(v_t)}{\sigma_\alpha^2}\right\} - v_t\left\{\frac{\alpha(v_t)}{\sigma_\alpha^2} + \frac{\mu}{\sigma_r^2}\right\} = -2v_t\frac{\mu}{\sigma_r^2}.$$

Therefore, $\frac{\partial\rho(A)}{\partial v_i} = 0$ if and only if $v_i = 0$ for $i \in \{r, t\}$. Consequently, the unique DFE is given by

$$E_0 = \left(\frac{1}{\gamma}\left(1 - \frac{\mu}{\overline{r}}\right), 0, 0, 0, 0\right).$$

Define the basic reproduction number for the evolutionary model (2.9) similar to the basic reproduction number of the non-evolutionary model (2.7), given in (2.3) but with trait dependency. That is,

$$\mathcal{R}_0 = \mathcal{R}_0(E_0) = \frac{\beta\omega}{\mu_p(\mu + \alpha(v_t) + \phi(v_r))} \cdot \frac{(r(v_r, v_t) - \mu)}{r(v_r, v_t)\gamma}\Big|_{E_0} = \frac{\beta\omega}{\mu_p(\mu + \overline{\alpha})} \cdot \frac{(\overline{r} - \mu)}{\overline{r}\gamma}. \tag{2.11}$$

Theorem 2.5. *Consider* (2.9) *with* $\mathcal{R}_0$ *given in* (2.11). *If* $\mathcal{R}_0 < 1$, *then the unique disease free equilibrium given by* $E_0 = \left(\frac{1}{\gamma}\left(1 - \frac{\mu}{\overline{r}}\right), 0, 0, 0, 0\right)$ *is locally asymptotically stable. If any of these inequalities is reversed,* E_0 *is a saddle and, therefore, unstable.*

Proof. The claim of uniqueness of the DFE follows from the previous discussion. To assess its stability, we calculate the Jacobian evaluated at E_0. For that, we notice that for $x, y \in \{S, I, P, v_r, v_t\}$, we have

$$\frac{\partial^2}{\partial y\partial x}(2\rho(A)) = \frac{\partial^2}{\partial y\partial x}\mathrm{tr}(A) + \frac{\left(\frac{\partial}{\partial y}\mathrm{tr}(A)\right)\left(\frac{\partial}{\partial x}\mathrm{tr}(A)\right) + \mathrm{tr}(A)\left(\frac{\partial^2}{\partial y\partial x}\mathrm{tr}(A)\right) - 2\left(\frac{\partial^2}{\partial y\partial x}\mathrm{det}(A)\right)}{\sqrt{(\mathrm{tr}(A))^2 - 4\mathrm{det}(A)}}$$
$$- \left\{\mathrm{tr}(A)\left(\frac{\partial}{\partial x}\mathrm{tr}(A)\right) - 2\left(\frac{\partial}{\partial x}\mathrm{det}(A)\right)\right\}\frac{\mathrm{tr}(A)\left(\frac{\partial}{\partial y}\mathrm{tr}(A)\right) - 2\left(\frac{\partial}{\partial y}\mathrm{det}(A)\right)}{\{(\mathrm{tr}(A))^2 - 4\mathrm{det}(A)\}^{\frac{3}{2}}}.$$

Since $v_i = 0$, for $i \in \{r, t\}$ and, therefore, $\frac{\partial}{\partial v_i}\mathrm{tr}(A)\Big|_{E_0} = \frac{\partial}{\partial v_i}\mathrm{det}(A)\Big|_{E_0} = 0$, as well as $\mathrm{det}(A)|_{E_0} = 0$ and $\mathrm{tr}(A)|_{E_0} = -(\mu + \overline{\alpha})$, we have

$$\frac{\partial^2}{\partial y\partial v_i}(2\rho(A))\Big|_{E_0} = \left(\frac{\partial^2}{\partial y\partial v_i}\mathrm{tr}(A)\right) - \frac{(\mu + \overline{\alpha})\left(\frac{\partial^2}{\partial y\partial v_i}\mathrm{tr}(A)\right) + 2\left(\frac{\partial^2}{\partial y\partial v_i}\mathrm{det}(A)\right)}{\mu + \overline{\alpha}}\Big|_{E_0}$$

$$= -2\frac{\left(\frac{\partial^2}{\partial y \partial v_i}\det(A)\right)}{\mu + \overline{\alpha}}\Big|_{E_0} \tag{2.12}$$

for $i \in \{r, t\}$. Since for $M \in \{S, I\}$, we have

$$\begin{aligned}
\frac{\partial}{\partial M}\left(\frac{\partial \det(A)}{\partial v_r}\right)\Big|_{E_0} &= \frac{\partial}{\partial v_r}\frac{\partial \det(A)}{\partial M}\Big|_{E_0} = \frac{\partial}{\partial v_r}\gamma r(v_r, v_t)(\mu + \alpha(v_t) + \phi(v_r) + \beta P)\Big|_{E_0} \\
&= \frac{-2\gamma v_r}{\sigma_r^2} r(v_r, v_t)(\mu + \alpha(v_t) + \phi(v_r) + \beta P) + \gamma r(v_r, v_t)\overline{\phi}\frac{2v_r}{\sigma_\phi^2} e^{-\frac{v_r^2}{\sigma_\phi^2}}\Big|_{E_0} = 0, \\
\frac{\partial}{\partial M}\left(\frac{\partial \det(A)}{\partial v_t}\right)\Big|_{E_0} &= \frac{\partial}{\partial v_t}\frac{\partial \det(A)}{\partial M}\Big|_{E_0} = \frac{\partial}{\partial v_t}\gamma r(v_r, v_t)(\mu + \alpha(v_t) + \phi(v_r) + \beta P)\Big|_{E_0} \\
&= \frac{-2\gamma v_t}{\sigma_r^2} r(v_r, v_t)(\mu + \alpha(v_t) + \phi(v_r) + \beta P) - \gamma r(v_r, v_t)\alpha(v_t)\frac{2v_t}{\sigma_\alpha^2}\Big|_{E_0} = 0, \\
\frac{\partial}{\partial P}\left(\frac{\partial \det(A)}{\partial v_r}\right)\Big|_{E_0} &= \frac{\partial}{\partial v_r}\frac{\partial \det(A)}{\partial P}\Big|_{E_0} = \frac{\partial}{\partial v_r} - \beta r(v_r, v_t)(1 - \gamma(S + I)) + \beta(\mu + \alpha(v_t))\Big|_{E_0} \\
&= \frac{2v_r}{\sigma_r^2}\beta\mu\Big|_{E_0} = 0, \\
\frac{\partial}{\partial P}\left(\frac{\partial \det(A)}{\partial v_t}\right)\Big|_{E_0} &= \frac{\partial}{\partial v_t}\frac{\partial \det(A)}{\partial P}\Big|_{E_0} = \frac{\partial}{\partial v_t} - \beta r(v_r, v_t)(1 - \gamma(S + I)) + \beta(\mu + \alpha(v_t))\Big|_{E_0} \\
&= \frac{2v_t}{\sigma_r^2}\beta\mu - \frac{2v_t}{\sigma_\alpha^2}\beta\mu\alpha(v_t)\Big|_{E_0} = 0,
\end{aligned}$$

we obtain, by (2.12),

$$\frac{\partial}{\partial M}\frac{\partial}{\partial v_i}\rho(A) = 0, \qquad i \in \{r, t\},\ M \in \{S, I, P\}.$$

Furthermore, using the expression of G_r and G_t in the Appendix, $\frac{\partial}{\partial v_r}\det(A) = v_r G_r(v_r, v_t)$ and $\frac{\partial}{\partial v_t}\det(A) = v_t G_t(v_r, v_t)$ so that, by the product rule and recalling that $v_r = 0$ and $v_t = 0$ at E_0, we have

$$\begin{aligned}
\frac{\partial^2}{\partial v_r^2}\det(A)\Big|_{E_0} &= G_r(v_r, v_t) + v_r\left(\frac{\partial}{\partial v_r}G_r(v_r, v_t)\right)\Big|_{E_0} = G_r(0, 0) \\
&= \left(\frac{2}{\sigma_r^2}\right)\mu(\mu + \overline{\alpha}) - \mu\overline{\phi}\frac{2}{\sigma_\phi^2} + \mu\overline{\phi}\frac{2}{\sigma_\phi^2} = \frac{2}{\sigma_r^2}\mu(\mu + \overline{\alpha}), \\
\frac{\partial^2}{\partial v_t \partial v_r}\det(A)\Big|_{E_0} &= v_r\left(\frac{\partial}{\partial v_t}G_r(v_r, v_t)\right)\Big|_{E_0} = 0, \\
\frac{\partial^2}{\partial v_t^2}\det(A)\Big|_{E_0} &= G_t(v_r, v_t) + v_t\left(\frac{\partial}{\partial v_t}G_t(v_r, v_t)\right)\Big|_{E_0} = G_t(0, 0) \\
&= \left(\frac{2}{\sigma_r^2}\right)\mu(\mu + \overline{\alpha}) + \mu\overline{\alpha}\frac{2}{\sigma_\alpha^2} - \mu\overline{\alpha}\frac{2}{\sigma_\alpha^2} = \left(\frac{2}{\sigma_r^2}\right)\mu(\mu + \overline{\alpha}).
\end{aligned}$$

Hence, by (2.12),

$$\frac{\partial^2}{\partial v_r^2}\rho(A)\Big|_{E_0} = -\frac{2\mu}{\sigma_r^2} \qquad \text{and} \qquad \frac{\partial^2}{\partial v_t^2}\rho(A)\Big|_{E_0} = -\frac{2\mu}{\sigma_r^2}.$$

Thus, the Jacobian at E_0 is therefore given by

$$J(E_0) = \begin{bmatrix} -(\overline{r}-\mu) & -(\overline{r}-2\mu) & -\frac{\beta}{\gamma}(1-\frac{\mu}{\overline{r}}) & 0 & 0 \\ 0 & -\mu-\overline{\alpha} & \frac{\beta}{\gamma}(1-\frac{\mu}{\overline{r}}) & 0 & 0 \\ 0 & \omega & -\mu_p & 0 & 0 \\ 0 & 0 & 0 & -2k\frac{\mu}{\sigma_r^2} & 0 \\ 0 & 0 & 0 & 0 & -2k\frac{\mu}{\sigma_r^2} \end{bmatrix}$$

with eigenvalues $-(\overline{r}-\mu), -2k\frac{\mu}{\sigma_r^2} < 0$ and the solutions to

$$\lambda^2 + (\mu+\overline{\alpha}+\mu_p)\lambda + (\mu+\overline{\alpha})\mu_p - \frac{\beta\omega}{\gamma}\left(1-\frac{\mu}{\overline{r}}\right) = 0.$$

By Descartes' rule of signs, there exists a unique positive solution if

$$(\mu+\overline{\alpha})\mu_p < \frac{\beta\omega}{\gamma}\left(1-\frac{\mu}{\overline{r}}\right) \qquad \Longleftrightarrow \qquad 1 < \frac{\beta\omega}{(\mu+\overline{\alpha})\mu_p}\cdot\frac{(\overline{r}-\mu)}{\gamma\overline{r}} = \mathcal{R}_0.$$

But if the inequality is reversed, then both solutions have negative real parts. This completes the claim. □

Theorem 2.6. *Consider* (2.9) *with* $\mathcal{R}_0$ *given in* (2.11). *Let* $E^* = (S^*, I^*, P^*, v_r^*, v_t^*)$ *be an endemic equilibrium, then* v_i^* *solves* $\frac{\partial\rho(A)}{\partial v_i} = 0$, *for* $i \in \{r, t\}$, *and*

$$S^* = S^*(v_r^*, v_t^*) = \frac{\mu_p(\mu+\alpha(v_t^*)+\phi(v_r^*))}{\beta\omega},$$

$$I^* = N^*(v_r^*, v_t^*) - S^*(v_r^*, v_t^*), \qquad \text{and} \qquad P^*(v_r^*, v_t^*) = \frac{\omega}{\mu_p}I^*(v_r^*, v_t^*),$$

where

$$N^*(v_r^*, v_t^*) = \frac{(r(v_r^*, v_t^*) - \mu - \alpha(v_t^*)}{2r(v_r^*, v_t^*)\gamma} + \frac{\sqrt{(r(v_r^*, v_t^*) - \mu - \alpha(v_t^*))^2 + 4r(v_r^*, v_t^*)\gamma\alpha(v_t^*)S^*(v_r^*, v_t^*)}}{2r(v_r^*, v_t^*)\gamma}.$$

If $\mathcal{R}_0 > 1$, *then there exist at least one endemic equilibrium* $E^* = (S^*(0,0), I^*(0,0), P^*(0,0), 0, 0)$.

Proof. The first claim follows immediately from the structure of the model. More precisely, for given v_r^*, v_t^* that solve $\frac{\partial\rho(A)}{\partial v_r} = \frac{\partial\rho(A)}{\partial v_t} = 0$, the equilibrium equations for the variables S, I, P are identical to the ones in the non-evolutionary case, but with parameters r, ϕ, α evaluated at v_r^*, v_t^*. Thus, S^*, I^*, P^* are given by Theorem 2.3, if $\mathcal{R}_0 > 1$. To complete the proof, we show that $v_r^* = v_t^* = 0$ solve $\frac{\partial\rho(A)}{\partial v_r} = \frac{\partial\rho(A)}{\partial v_t} = 0$. Note that $\frac{\partial}{\partial v_i}\det(A) = v_i G_i(v_r, v_t)$ and $\frac{\partial}{\partial v_i}\mathrm{tr}(A) = v_i F_i(v_r, v_t)$ (see Appendix), so that for $v_i = 0$, $\frac{\partial}{\partial v_i}\mathrm{tr}(A) = \frac{\partial}{\partial v_i}\det(A) = 0$ for $i \in \{r, t\}$. Hence, by (2.10), independent of the sign of $(\mathrm{tr}(A))^2 - 4\det(A)$, $\frac{\partial\rho(A)}{\partial v_i} = 0$ for $i \in \{r, t\}$. Hence, for $\mathcal{R}_0 > 1$, there exists an endemic equilibrium with $v_r^* = v_t^* = 0$ and

$$S^* = S^*(0,0) = \frac{\mu_p(\mu+\overline{\alpha})}{\beta\omega}$$

and $I^* = N^*(0,0) - S^*(0,0)$, $P^*(0,0) = \frac{\omega}{\mu_p} I^*(0,0)$ with

$$N^*(0,0) = \frac{\overline{r} - \mu - \overline{\alpha} + \sqrt{(\overline{r} - \mu - \overline{\alpha})^2 + 4\overline{r}\gamma\overline{\alpha}S^*(0,0)}}{2\overline{r}\gamma}.$$

□

Theorem 2.7. *Targeting the pathogen transmission rate, shedding rate, decay rate, or the host density-dependent suppression are equally effective at reducing $\mathcal{R}_0$. Furthermore, although resistance always decreases $\mathcal{R}_0$, tolerance can increase $\mathcal{R}_0$ when the epidemiological benefits of keeping hosts alive for longer outweigh the demographic costs of reduced reproduction.*

Proof. The normalized forward sensitivity index is used to capture how a relative change in a parameter impacts a relative change in a variable of interest [26–28]. In our context, we are interested in

$$\Gamma_x^{\mathcal{R}_0} = \frac{\partial \mathcal{R}_0}{\partial x} \frac{x}{\mathcal{R}_0},$$

where $\mathcal{R}_0$ is given in Eq (2.11). By plugging in the corresponding expressions for β, ω, μ_P, and γ, we find that $\Gamma_\beta^{\mathcal{R}_0} = \Gamma_\omega^{\mathcal{R}_0} = 1$ and that $\Gamma_{\mu_p}^{\mathcal{R}_0} = \Gamma_\gamma^{\mathcal{R}_0} = -1$. This means that a 1% increase in pathogen transmission or shedding leads to a 1% increase in $\mathcal{R}_0$ and, conversely, a 1% increase in pathogen decay or host density-dependent suppression leads to a 1% decrease in $\mathcal{R}_0$.

We can also calculate the normalized forward sensitivity index for resistance and tolerance:

$$\begin{aligned}
\Gamma_{v_r}^{\mathcal{R}_0} &= \frac{\beta\omega}{\mu_p\gamma}\left[\left(\frac{r(v_r,v_t)-\mu}{r(v_r,v_t)}\right)\frac{\partial}{\partial v_r}\left(\frac{1}{\mu+\alpha(v_t)+\phi(v_r)}\right)+\left(\frac{1}{\mu+\alpha(v_t)+\phi(v_r)}\right)\frac{\partial}{\partial v_r}\left(\frac{r(v_r,v_t)-\mu}{r(v_r,v_t)}\right)\right]\frac{v_r}{\mathcal{R}_0} \\
&= \frac{\beta\omega}{\mu_p\gamma}\left[-\left(\frac{r(v_r,v_t)-\mu}{r(v_r,v_t)}\right)\frac{1}{(\mu+\alpha(v_t)+\phi(v_r))^2}\frac{\partial\phi(v_r)}{\partial v_r}+\left(\frac{1}{\mu+\alpha(v_t)+\phi(v_r)}\right)\frac{\mu}{r(v_r,v_t)^2}\frac{\partial r(v_r,v_t)}{\partial v_r}\right]\frac{v_r}{\mathcal{R}_0} \\
&= v_r\left[-\frac{\phi'(v_r)}{\mu+\alpha(v_t)+\phi(v_r)}+\frac{\mu\frac{\partial r(v_r,v_t)}{\partial v_r}}{r(v_r,v_t)(r(v_r,v_t)-\mu)}\right].
\end{aligned}$$

Since $\phi(v_r)$ is monotonically increasing in $v_r \geq 0$ and $r(v_r, v_t)$ is monotonically decreasing in $v_r \geq 0$, this quantity is strictly negative. Thus, the evolution of resistance will always decrease $\mathcal{R}_0$. Similarly, for tolerance, we have

$$\Gamma_{v_t}^{\mathcal{R}_0} = v_t\left[-\frac{\alpha'(v_t)}{\mu+\alpha(v_t)+\phi(v_r)}+\frac{\mu\frac{\partial r(v_r,v_t)}{\partial v_t}}{r(v_r,v_t)(r(v_r,v_t)-\mu)}\right].$$

In this case, both $\alpha(v_t)$ and $r(v_r, v_t)$ are monotonically decreasing in v_t, meaning that tolerance can increase $\mathcal{R}_0$ if the epidemiological benefits of keeping hosts alive for longer outweighs the ecological costs of reducing overall host density: $\frac{\alpha'(v_t)}{\mu+\alpha(v_t)+\phi(v_r)} < \frac{\mu\frac{\partial r(v_r,v_t)}{\partial v_t}}{r(v_r,v_t)(r(v_r,v_t)-\mu)}$. □

Similar to the study in Figure 1 for the ecological model (2.1), we can investigate the dynamics with increasing $\mathcal{R}_0$ for our eco-evolutionary model. Figure 1 already revealed that the classical result

that $\mathcal{R}_0$ serves as the threshold between the convergence of the disease-free and an endemic equilibrium is violated. Although a transcritical bifurcation occurred at $\mathcal{R}_0 = 1$, the endemic equilibrium lost stability through a Hopf bifurcation with increasing values of $\mathcal{R}_0$ for the parameter values used in Figure 1. However, once the evolution of host defense mechanisms is included, we observe the disappearance of the Hopf bifurcation within a large $\mathcal{R}_0$ regime for the same parameter values (Figure 2). This suggests that the evolution of traits can have a stabilizing effect for the system, making it less vulnerable to stochastic fluctuations that, for large oscillations, can result in the extinction of the species. Thus, although purely ecological models of host-parasite interactions may predict long-term oscillatory behavior under certain parameter regimes, the evolution of resistance and tolerance act as stabilizing forces, leading to the disappearance of the Hopf bifurcation: the classical instabilities described in earlier work [14] may be suppressed by the adaptive response of the host population. Figure 2 further reveals the non-monotonicity of the variables I and P with respect to $\mathcal{R}_0$ at the endemic equilibrium. Once $\mathcal{R}_0 > 1$, an endemic equilibrium with variables $S^*(\mathcal{R}_0), I^*(\mathcal{R}_0), P^*(\mathcal{R}_0)$ occurs and attracts the orbit. While $S^*(\mathcal{R}_0)$ continues to decrease monotonically in $\mathcal{R}_0$, $I^*(\mathcal{R}_0)$ and $P^*(\mathcal{R}_0)$ initially increase, due to the evolution of tolerance, before monotonically decreasing. The drastic decline in the equilibrium value of the susceptible population as $\mathcal{R}_0$ increases is particularly concerning from a management perspective.

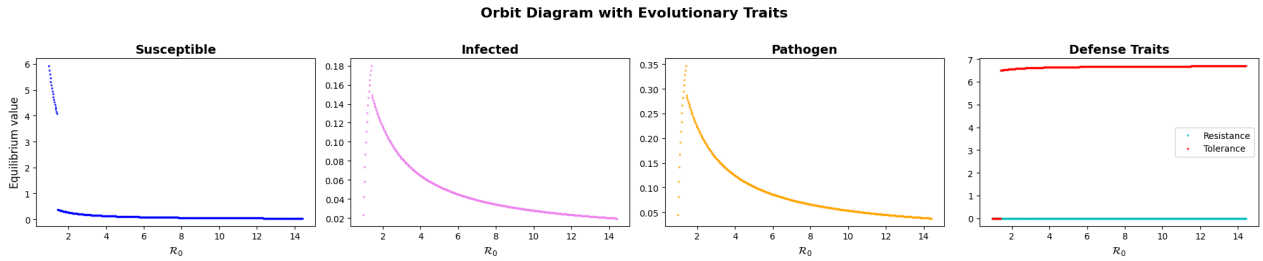

Figure 2. Orbit diagram for eco-evolutionary dynamics with increasing values of $\mathcal{R}_0$. The parameter values are the same as in Figure 1. In contrast to Figure 1, no Hopf bifurcation is observed. Instead, for $\mathcal{R}_0 > 1$, the solution converges to an endemic equilibrium, where I^*, P^*, as functions of $\mathcal{R}_0$ reach their maximum values for a critical value $\overline{\mathcal{R}}_0$.

Another aspect not observed in the purely ecological model (2.1) is the existence of bistable regions. By considering different initial tolerance levels, we found bistability between two endemic equilibria, one for which both strategies do not evolve $v_r^* = v_t^* = 0$ and another endemic equilibrium where tolerance evolves so that $v_r^* = 0$ and $v_t^* > 0$ (Figure 3). The existence of such bistability is reasonable as for low $v_t(0)$ and low/moderate R_0, low levels of pathogen exist in the population as mortality is likely and rapid once a host is infected with a virus, thereby hampering transmission. Due to this, the costs of evolving tolerance outweigh the individual benefits of persisting with the virus. Despite the same R_0, in populations with moderate to high initial levels of tolerance, the pathogen can spread more effectively in the population. Due to the reservoir of hosts that permit high levels of circulating virus, it is advantageous for individuals to evolve tolerance as they are likely to encounter the virus. Although resistance eventually disappears in both strategies, there is a transient increase in resistance for hosts with moderate initial tolerance levels. This is because low initial levels immediately choose the "no defense" strategy and high-tolerance individuals suffer negligible mortality from the virus. However, moderate-tolerance hosts experience a transient spike in resistance to buffer mortality, before tolerance

evolves sufficiently and resistance diminishes. As the current paper focuses on how naive hosts can evolve defense mechanisms under a range of environmental contexts and host-pathogen properties, we save deeper exploration of this bistability for future work.

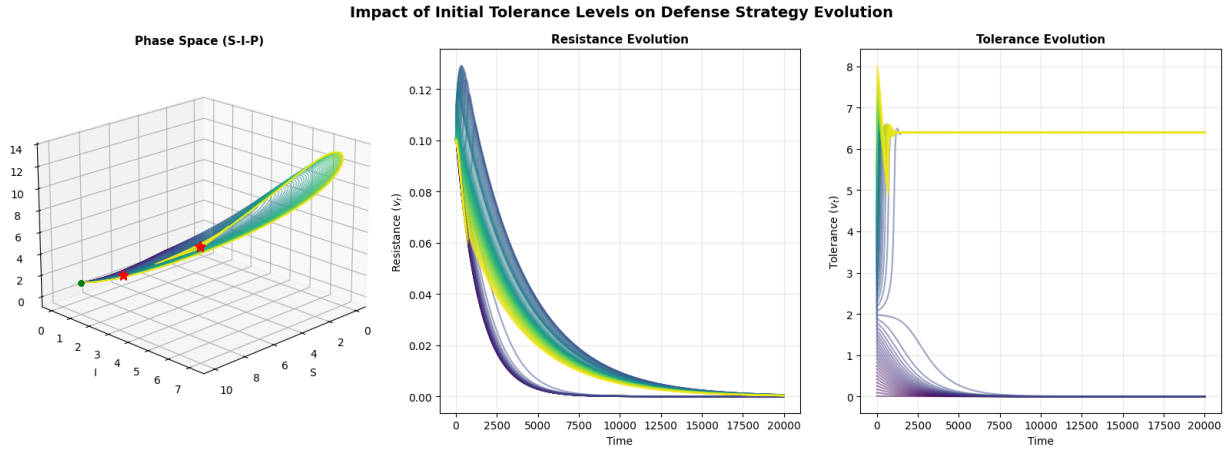

Figure 3. Latin hypercube sampling that samples initial tolerance levels and fixes $S_0 = 10$, $I_0 = 1$, $P_0 = 2$, and $v_r = 0.1$. Parameters used are the same as in Figure 1 with $\beta = 0.1$, resulting in $R_0 = 1.03$. Two strategies appear: one associated with no evolved defense mechanism and another associated with tolerance.

3. Factors that shape the evolution of host defenses

In this section, we computationally explore the effects of varying parameters associated with host and pathogen life history and environmental properties on the evolution of the host's preferred defense strategy. To allow for comparison across the different scenarios, we choose, unless stated differently, model (2.9) with the parameter values given in Table 1.

3.1. Impact of pathogenic properties on evolution of defense mechanisms

Next, we perform simulations of our Darwinian epizootic model to investigate the impact of pathogenic infection on the evolution of host defense mechanisms. The baseline parameters we use are given in Table 1. These parameter values were chosen to be broadly plausible across various host-pathogen systems, numerically convenient for simulation, and illustrative of differences in evolutionary dynamics across parameter ranges. They are not intended to represent any single biological system precisely, but are rather meant to demonstrate how properties of the environment, host, and pathogen can theoretically shape the evolution of defense mechanisms. It is worth specifically commenting on our evolvability parameter, k. This parameter, along with the selection gradient, determines the evolutionary speed of host defense mechanisms and thereby influences the extent of coupling between the ecological and evolutionary dynamics. Larger values of k promote faster evolution relative to ecological processes, whereas smaller values enforce greater timescale separation, paralleling classical adaptive dynamics formulations. The value of $k = 10$ was merely chosen for numerical efficiency and greatly speeds up simulation times–using lower values of k, which more accurately captures the time scale separation between evolutionary and ecological

dynamics in our setting, was inordinately expensive computationally. However, our simulations of the main results in the manuscript show that using lower values of k only increases the time to reach the eco-evolutionary equilibrium but does not impact the final evolutionarily stable strategies.

Table 1. Baseline model parameters and values used in simulations.

Parameter	Interpretation	Value
$\overline{r}$	Baseline intrinsic growth rate	1/year
γ	Density-dependent growth suppression	0.1/organism
μ	Intrinsic death rate	0.1/year
β	Transmission rate	0.1/year
$\overline{\phi}$	Baseline recovery rate	1/year
$\overline{\alpha}$	Baseline disease-induced death rate	0.15/year
ω	Pathogen shedding rate	0.35/year
μ_p	Pathogen decay rate	0.3/year
σ_r^2	Impact of defense mechanisms on intrinsic growth rate	50
σ_α^2	Impact of defense mechanisms on pathogen-induced death rate	10
σ_ϕ^2	Impact of defense mechanisms on recovery rate	10
k	Evolvability	10
$S(0)$	Initial susceptible host population	10
$I(0)$	Initial infected host population	1
$P(0)$	Initial pathogen population	2
$v_r(0)$	Initial resistance trait	0.1
$v_t(0)$	Initial tolerance trait	0.1

We first explore how pathogen load impacts the evolution of host defense mechanisms by simulating three conditions: no pathogen shedding ($\omega = 0$), low pathogen shedding ($\omega = 0.2$), and high pathogen shedding ($\omega = 0.5$) (Figure 4). When $\omega = 0$, the pathogen is rapidly eliminated from the population, and neither resistance nor tolerance evolves–since the cost of defense exceeds the benefit, v_r and v_t evolve towards 0. Calculating $\mathcal{R}_0$, as given in (2.11), yields $\mathcal{R}_0 = 0 < 1$. By Theorem 2.5, E_0 is LAS. In fact, the top row of Figure 5 suggests that E_0 is globally asymptotically stable. Under a low pathogen load, resistance mechanisms that allow infected individuals to recover rapidly are favored as repeated infections are unlikely. Here, $\mathcal{R}_0 = 2.4$ and, by Theorem 2.5, E_0 is unstable. When pathogens persist at high levels, evolving resistance is an ineffective long-term strategy, as hosts cannot avoid becoming infected by the pathogen for long. As such, tolerance is the favored defense mechanism. In this case, $\mathcal{R}_0 = 6$. Interestingly, there exists more than one pandemic equilibrium in the evolutionary case as indicated by the differences in limiting behavior of the variables v_r and v_t. At low pathogen shedding rates, the endemic equilibrium is at $v_t^* = 0$ while for high pathogen shedding rates, the endemic equilibrium is at $v_t^* > 0$. Based on Theorem 2.6, the number of equilibria is determined by the number of pairs (v_r, v_t) that solve $\frac{\partial}{\partial v_i}\rho(A) = 0$ for $i \in \{r, t\}$. Using the values utilized for Figure 4, we numerically find three endemic equilibria for $\omega = 0.2$ and three for $\omega = 0.5$. These endemic equilibria are located at boundaries such that at least one of the

variables v_r^*, v_t^* is zero. More precisely, when $\omega = 0.2$, we get $E_1^* \approx (3.75, 4.44, 2.96, 0, 0)$ with eigenvalues $\lambda \approx -0.72 \pm 0.18i, 0.27, -0.14, 0.05$, $E_2^* \approx (2.04, 6.27, 4.18, 0, 3.78)$ with eigenvalues $\lambda \approx -0.63 \pm 0.09i, -0.20, -0.09, 0.05$, and $E_3^* \approx (7.65, 1.09, 0.73, 1.74, 0)$ with eigenvalues $\lambda \approx -0.83 \pm 0.09i, -0.06 \pm 0.06i, -0.02$. Thus, only E_3^* is locally asymptotically stable, so that the resistance strategy $v_r^* = 1.74$ is preferred. For $\omega = 0.5$, we again obtain three endemic equilibria: $E_1^* \approx (1.5, 6.29, 10.48, 0, 0)$ with eigenvalues $\lambda = -1 \pm 0.13i, -0.25, 0.14, 0.11$, $E_2^* \approx (0.77, 7.48, 12.46, 0, 4.08)$ with eigenvalues $\lambda = -1.36, -0.60, -0.27, -0.13, -0.01$, and $E_3^* \approx (3.83, 4.19, 6.99, 2.22, 0)$ with eigenvalues $\lambda = -1.35, -0.76, -0.21, -0.08, 0.07$. Note that only E_2^* is locally asymptotically stable. This suggests, together with the Figure 5, that the respective equilibria for $\omega = 0.2$ and $\omega = 0.5$ are globally asymptotically stable. We remark that due to the complexity of $\frac{\partial}{\partial v_i}\rho(A)$, which involved the W-Lambert function in v_i, no explicit formula for v_i^* could be obtained. Through the investigation of intersections of contour plots, we confirmed that for the considered parameter combinations in Figure 4, no interior equilibrium (i.e., $v_i^* > 0$ for $i \in \{r, t\}$) exists.

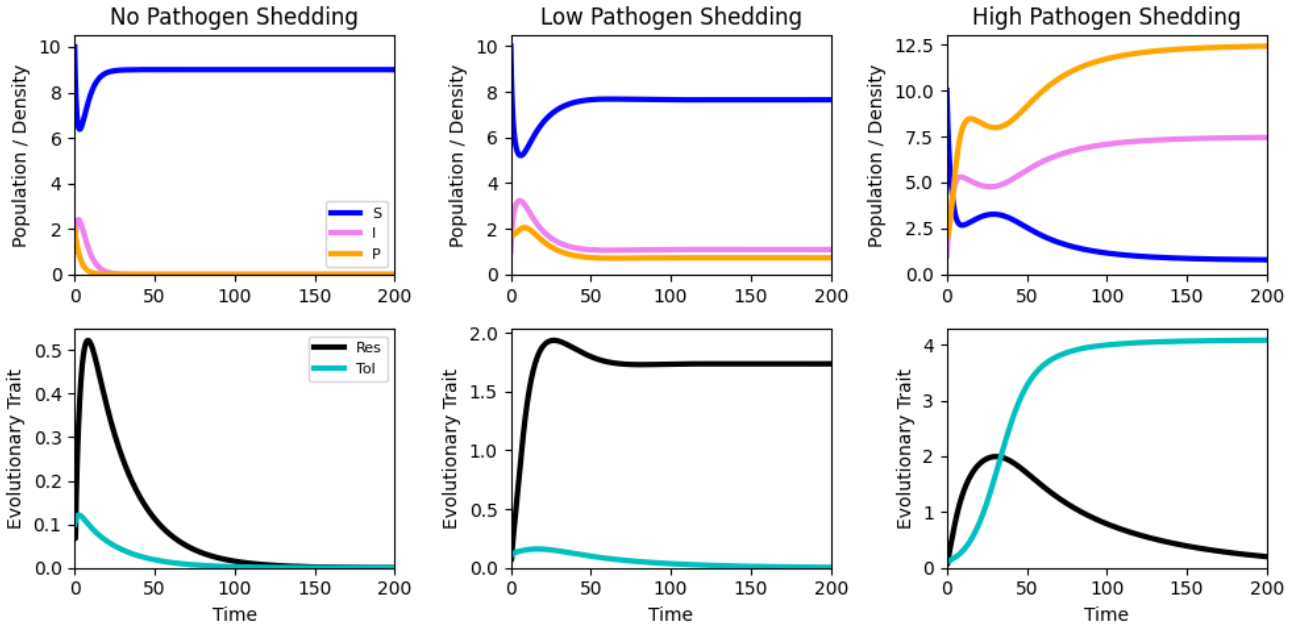

Figure 4. Impact of pathogen load on host-pathogen eco-evolutionary dynamics. Negligible pathogen burden leads to the evolution of neither resistance nor tolerance. A low pathogen burden promotes resistance, whereas a high pathogen burden promotes tolerance.

The evolutionary trajectories of host defense mechanisms over time can also be visualized on adaptive landscapes, which plot the fitness of the host as a function of its resistance and tolerance strategies (Figure 6). The adaptive landscape is used to capture how fitness changes with different trait values or strategies in a population [11, 12, 20]. Each point on the landscape represents a particular trait and its height corresponds to the fitness associated with that trait, here measured by the spectral bound of the transition matrix A. The slope of the landscape at any position indicates the direction and intensity of natural selection acting on the trait. As per Darwinian model construction, the pair of strategies evolves towards the peak of the adaptive landscape (analytically confirmed by verifying that

$\frac{d^2G}{dv^2} < 0$), which occurs at $G = \rho(A) = 0$ at an eco-evolutionary equilibrium. The uniqueness of this peak indicates a global maximum, indicating that no other combination of defense strategies is evolutionary beneficial.

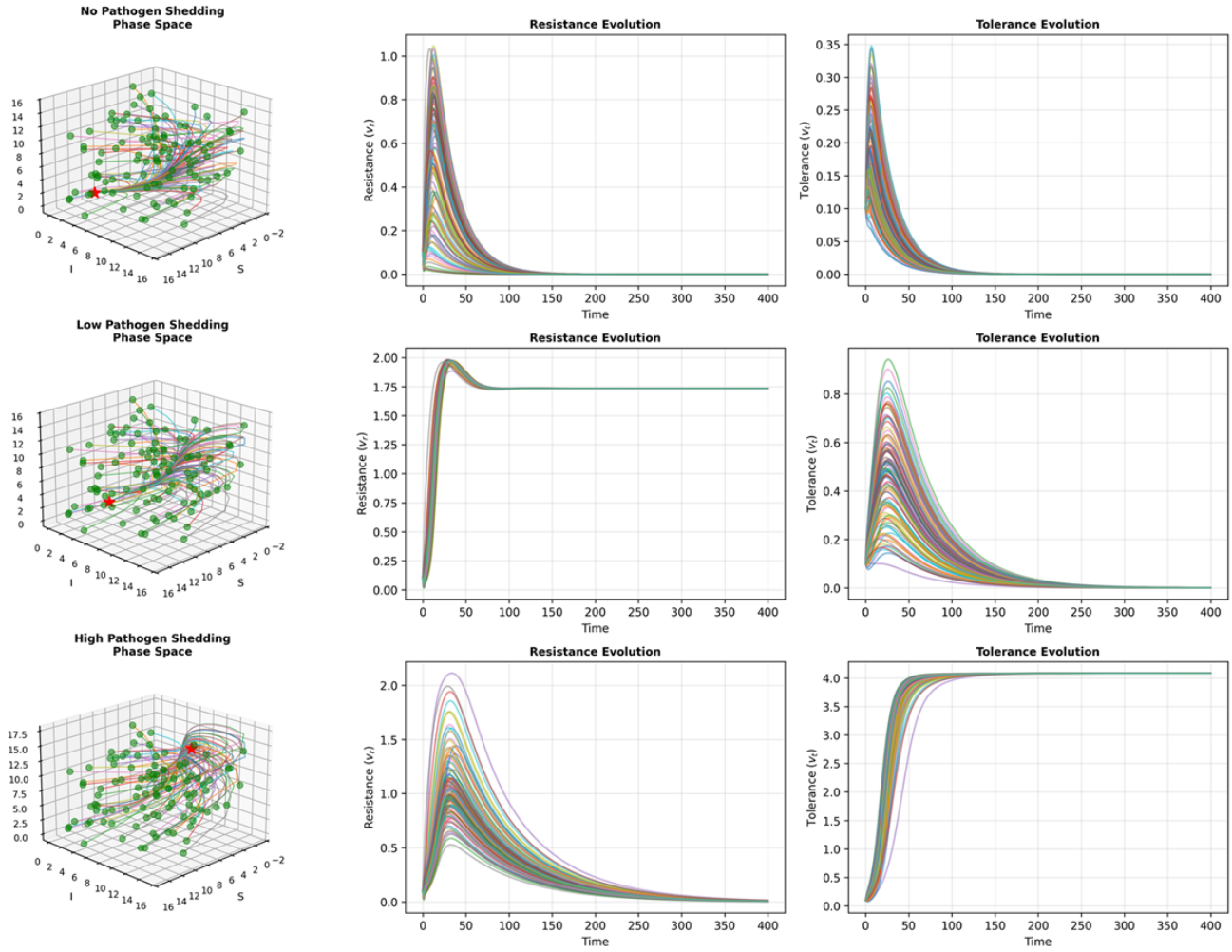

Figure 5. Latin hypercube sampling of initial susceptible, infected, and pathogen population sizes between [0.1,15] for low initial resistance and tolerance levels numerically suggests that the only eco-evolutionary equilibrium that is locally asymptotically stable is in fact globally asymptotically stable.

To further explore the impact of pathogen properties on host defenses, we present orbit diagrams of the variables v_t, v_r over a range of pathogen shedding rates, mortality rates, and transmission rates (Figure 7). These show the limiting values (numerical equilibria) of v_r and v_t across the different scenarios, using, except for the varying parameter, values as in Table 1. In accordance with our earlier simulation results, the higher the pathogen load (achieved either by higher pathogen shedding rates or lower pathogen mortality rates) or transmission rate, the more tolerance is favored over resistance as the dominant host defense mechanism. This can be explained by the realization that in these cases, the host cannot effectively avoid becoming infected for long, therefore favoring a long-term defense strategy.

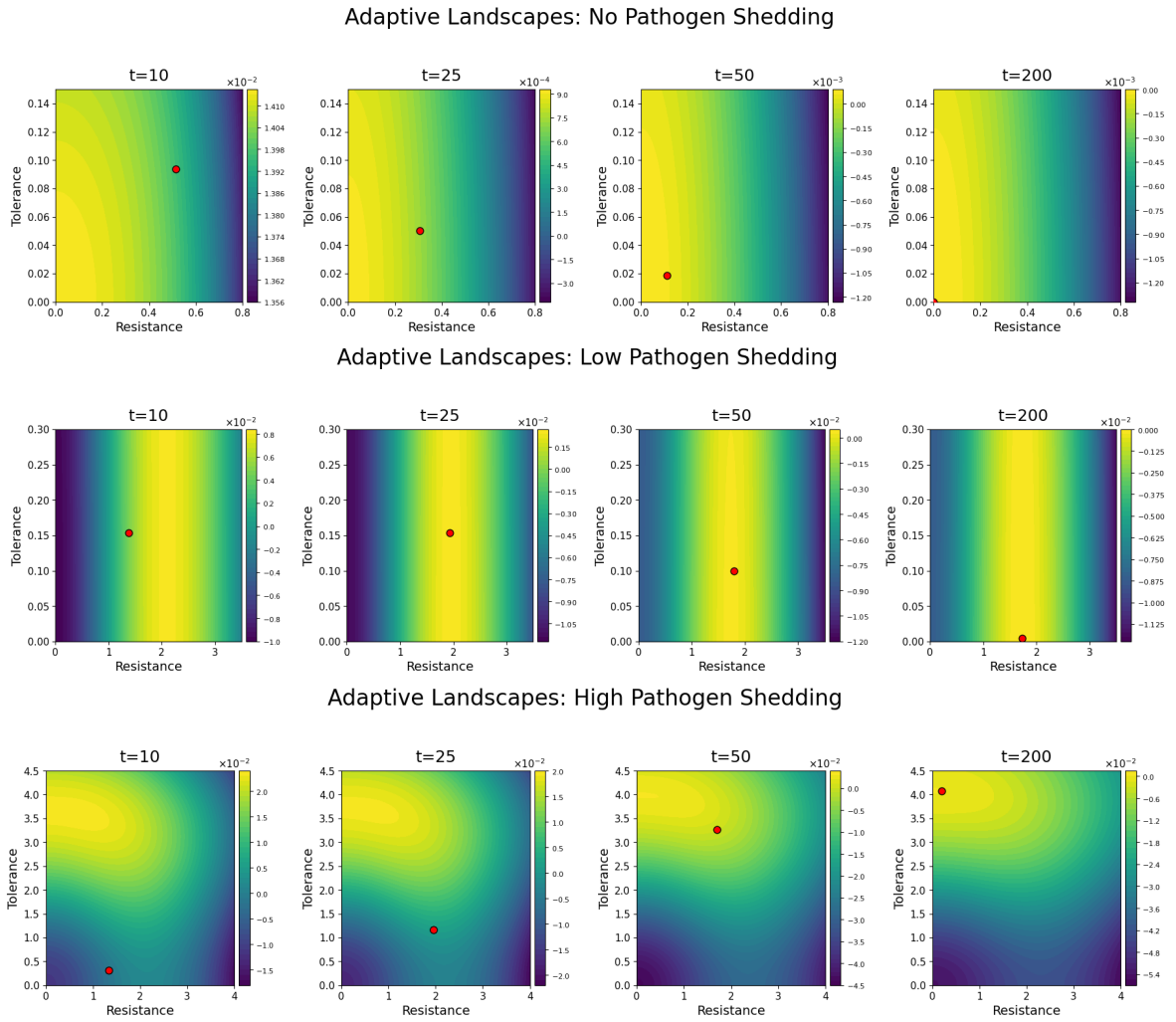

Figure 6. Adaptive landscapes for low and high pathogen shedding rates.

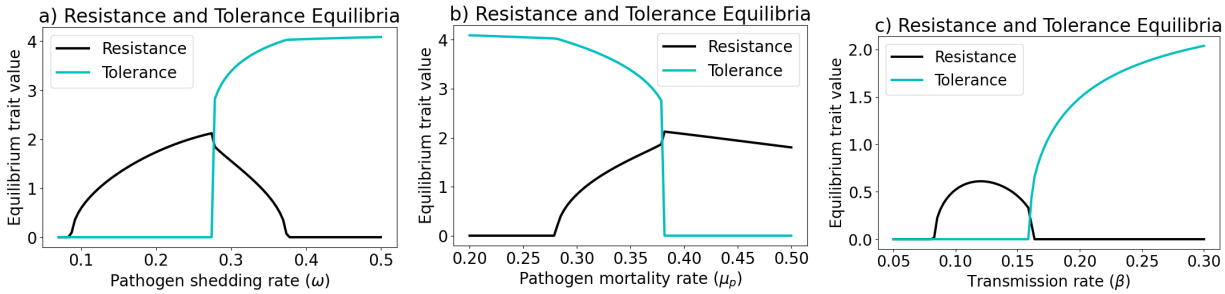

Figure 7. Impact of a) pathogen shedding, b) mortality, and c) transmission rates on host defense mechanisms. As pathogen load and transmission increase, the host favors the evolution of tolerance over resistance.

To complete our discussion on how pathogenic properties influence the evolution of defense mechanisms, we note that σ_ϕ is indirectly linked to pathogen evolution. Namely, if the host evolves resistance, the pathogen is likely to evolve in a way that counteracts the host's enhanced recovery.

This allows the pathogen to persist (and proliferate) in the host for longer, thereby enhancing its fitness. Given our proposed functional form of ϕ, an increase in σ_ϕ has a similar effect (Figure 8(a)). This can lead hosts to favor a tolerance rather than a resistance strategy (Figure 8(b)). Note that this exploration does not explicitly consider coevolutionary dynamics, as we do not consider the reciprocal relation of the host and pathogen, an interesting problem for future work. We remark that since immune tolerance is non-serotype-specific and does not directly affect pathogen growth or shedding, selection pressures on pathogen coevolution are minimal. Thus, we do not investigate the impact of σ_a on the evolution of host defense strategies.

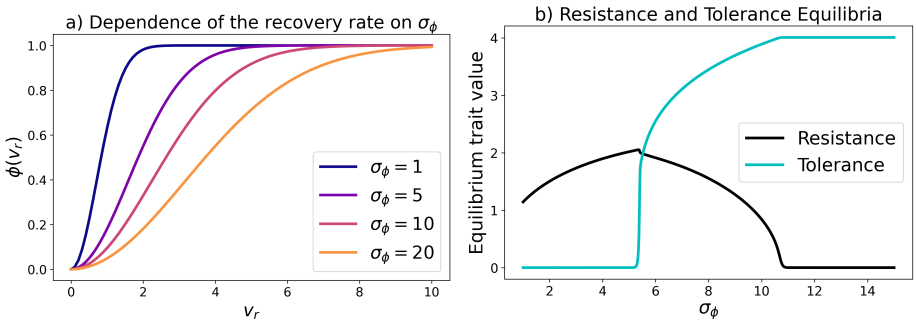

Figure 8. Impact of σ_ϕ on the a) recovery rate $\phi(v_r)$ and on the b) evolution of the host's defense mechanism. As σ_ϕ increases, the dominant defense mechanism can change from resistance to tolerance.

3.2. Impact of life history properties on evolution of defense mechanisms

Similarly, we can analyze the impact of host properties–the (maximal) reproductive rate $\bar{r}$, natural death rate μ, and intra-specific competition factor γ–on the evolution of defense strategies. As the natural death rate μ increases, the equilibrium value of the host population naturally decreases to lower levels and the preferred defense strategy changes (Figure 9). At low values of the natural death rate, the population evolves towards a tolerance-dominated strategy, as illustrated in the last column of Figure 9. Increasing the natural death rate eventually favors a resistance strategy. But at values beyond a critical threshold of the natural death rate, the decline factors dominate and can no longer be balanced by a defense strategy. In this case, the species survives by increasing its reproductive strength at the cost of an additional decline. Such evolutionary changes are also relevant when considering hunting, as hunting has similar effects to increased natural mortality rates in our model. Thus, increased hunting rates can indeed impact the species' defense strategy. For example, a species such as southern deer that has evolved towards a resistance strategy may start to favor increased reproduction at the cost of evolving no defense strategy, making it potentially more vulnerable to future pathogen exposure.

The opposite effect is obtained when increasing the reproductive rate $\bar{r}$ (Figure 10). With a higher reproduction rate, the selection pressure on species to evolve a defense strategy exceeds the selection pressure to evolve even higher intrinsic growth rates. For moderate reproductive values, a resistance defense strategy is favored as these species are less able to compensate for disease-induced death. However, as reproductive rates increase further, tolerance is favored, as rapidly-growing populations can better withstand persistent pathogen circulation and readily replace lost individuals. These findings are particularly relevant for populations that encounter new environments with elevated intrinsic growth

rates, for example, plants experiencing greater nutrient availability due to eutrophication or irrigation or domesticated animals selectively bred for maximal reproductive output. The opposite effect is observed for an increase in the density-dependent growth suppression (Figure 11). This is consistent, as an increase in γ results in the overall reduction of the growth contribution.

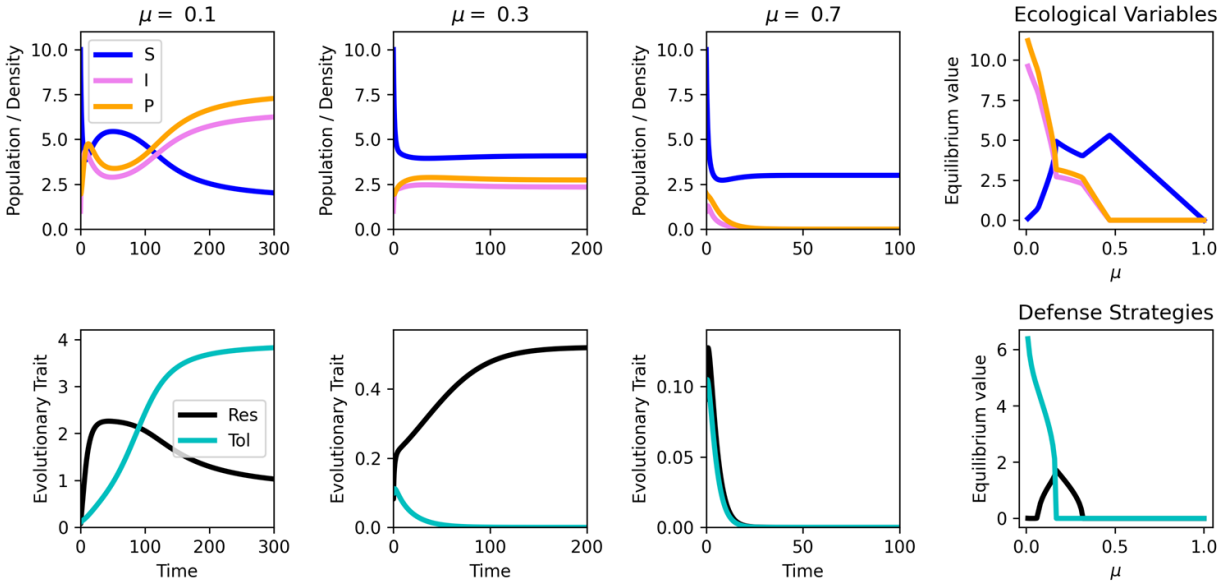

Figure 9. Impact of natural death rate on host-pathogen eco-evolutionary dynamics. Low natural death rates favor the evolution of tolerance, moderate natural death rates favor the evolution of resistance, and high natural death rates favor the evolution of neither.

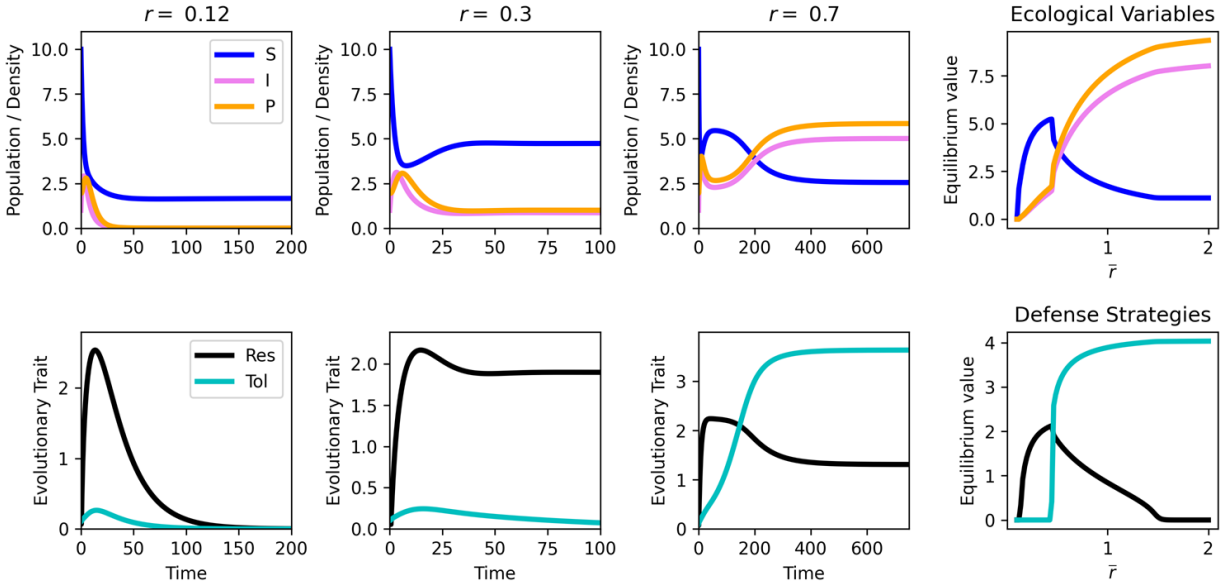

Figure 10. Impact of reproductive rate on host-pathogen eco-evolutionary dynamics. High reproductive rates favor the evolution of tolerance, moderate growth rates favor the evolution of resistance, and low reproductive rates favor the evolution of neither.

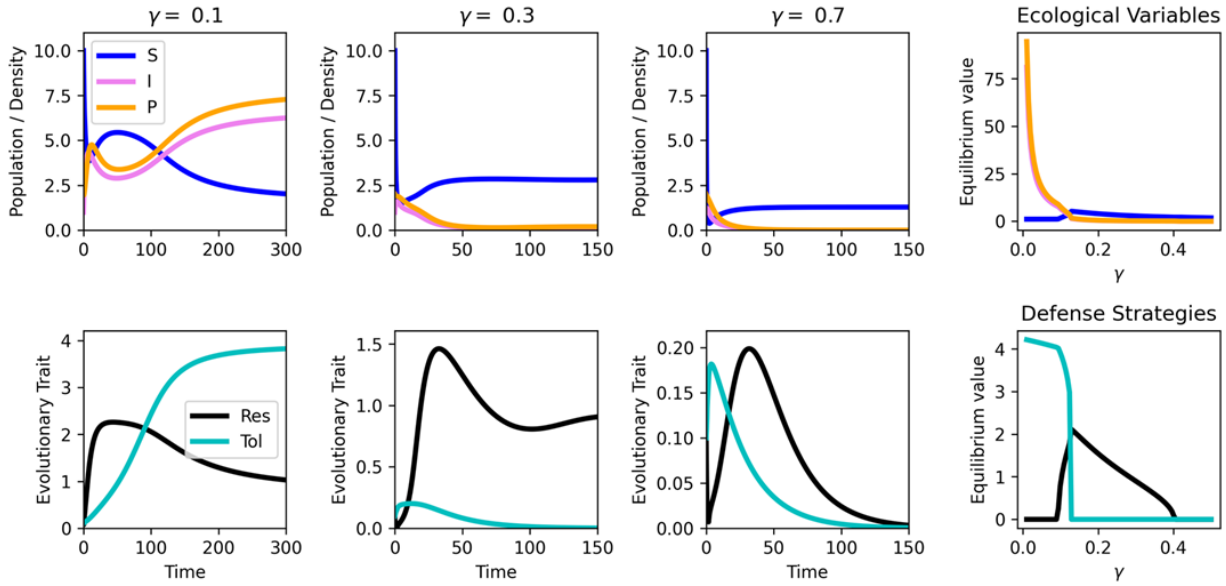

Figure 11. Impact of density-dependent growth suppression on host-pathogen eco-evolutionary dynamics. Low density-dependent growth suppression favors the evolution of tolerance, moderate growth suppression favors the evolution of resistance, and high growth suppression favors the evolution of neither.

3.3. Impact of environment on evolution of defense mechanisms

With a broad understanding of how pathogen characteristics influence host defense mechanisms, we now specifically focus on EHD. Our goal is to determine why white-tailed deer in northern regions, white-tailed deer in southern regions, and cattle in Africa display such distinct responses to this disease. We hypothesize that these differences stem from variations in EHDV seasonality across environments. Northern deer experience cooler temperatures and shorter summers than their southern counterparts, while African cattle, though subject to seasonal fluctuations, experience EHDV as an endemic infection.

To test this hypothesis, we model the transmission rate as a periodic function of time to represent seasonal variation. To study the impact of the length and intensity of the season, we represent the seasonal transmission rate $\beta(t) = \overline{\beta} + s(t)$ as dependent on a base level $\overline{\beta}$ and a seasonal contribution function $s(t) = h \cdot \sin\left(\frac{\pi}{\ell} \cdot \left(t \bmod 1 - \left(0.5 - \frac{\ell}{2}\right)\right)\right)$ if $|(t \bmod 1) - 0.5| < \frac{\ell}{2}$ and $s(t) = 0$ otherwise. By construction, $s(t)$ depends on ℓ and h, representing the length and height of the summer season, respectively (Figure 12(a)). For our purposes, to discuss the evolution of defense mechanisms to EHD in different environments, we focus on specific model parameters representing a northern, southern, and African environment (Figure 12(b)).

Including seasonality in the transmission rate of our Darwinian epizootic model presents an additional challenge, as the previously autonomous structure is lost. Instead, a nonautonomous (albeit periodic) version of (2.9) must be considered. Due to the periodic nature of the differential system, the spectral bound of the population projection matrix is no longer the appropriate fitness metric. As shown in prior work [29], we must instead consider a fitness function that incorporates the periodic

information and, therefore, express the fitness in terms of the dominant Floquet exponent. This allows the computation of fitness *across* seasonal cycles. Practically, to compute the Floquet exponents, we integrate our system over one period and derive the monodromy matrix from which the Floquet exponents are computed. To implement evolutionary dynamics, we perturb the strategy v_i in both directions, $v_i + \epsilon$ and $v_i - \epsilon$, compute the maximal Floquet exponent for their respective matrix differential systems, calculate the difference, normalize by the size of the perturbation, and multiply by the evolvability of the trait:

$$\Delta v_i = k\frac{\mu(\mathbf{A}(v_i + \epsilon)) - \mu(\mathbf{A}(v_i - \epsilon))}{2\epsilon}.$$

This formulation allows the analysis of the effect of seasonal variations in the transmission rate on the preferred defense strategies. We find that for sufficiently small seasonal variations (small height and small length), the host does not evolve a defense strategy and therefore maximizes its reproduction (Figure 13). However, as the height or the length of the season increases, the host starts evolving a defense mechanism at the cost of reproduction. For medium levels of the season, a resistance strategy is preferred (i.e., $v_t - v_r < 0$), whereas for sufficiently high seasonal values, a tolerance strategy dominates (i.e., $v_t - v_r > 0$).

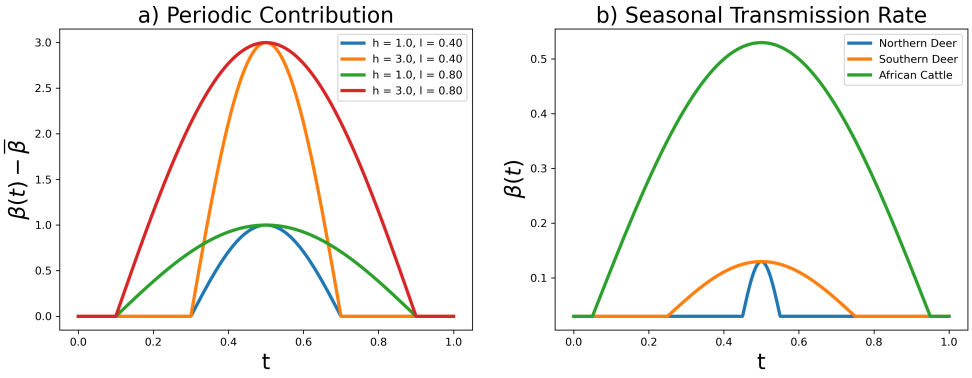

Figure 12. Considering a seasonal transmission rate $\beta(t) = \overline{\beta} + s(t)$ with fixed $\overline{\beta} = 0.03$ and varying seasonality characteristics. a) Visualization of the seasonality contribution $s(t)$ as a function of height h and length ℓ of the summer season. b) Considered cases, representing seasonal variation of EHDV in northern ($h = 0.1, l = 0.1$), southern ($h = 0.1, l = 0.5$), and African environments ($h = 0.5, l = 0.9$).

More specifically, we can use the periodic transmission rate formulation, as suggested in Figure 12(b), to simulate the seasonal dynamics experienced by northern deer, southern deer, and African cattle (Figure 14). Changes in the environmental conditions experienced by deer and cattle are sufficient to drive variation in host defense strategies. Northern deer, exposed to low and infrequent EHDV transmission, evolve neither resistance nor tolerance. In contrast, southern deer, facing moderate and more prolonged transmission, evolve resistance, whereas African cattle, experiencing high and endemic levels of EHDV, evolve tolerance. In future work, we plan to build on these results to investigate the impact of climate change by examining the effects of extreme weather events and high temperatures on pathogen reproduction and viability.

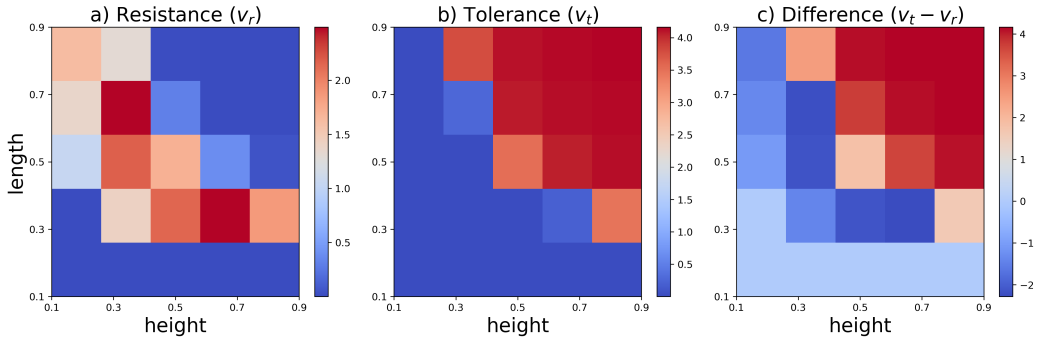

Figure 13. Preferred strategy, tolerance vs. resistance, in the presence of a seasonally varying transmission rate. A resistance strategy only evolves for medium levels of height and length of the season (a), while a tolerance strategy evolves for sufficiently high values of length and height (b). If the summer season is short and/or cold, no defense mechanism is lucrative. Dependent on the length and intensity of the summer season, the dominance of one of the strategies strengthens (c).

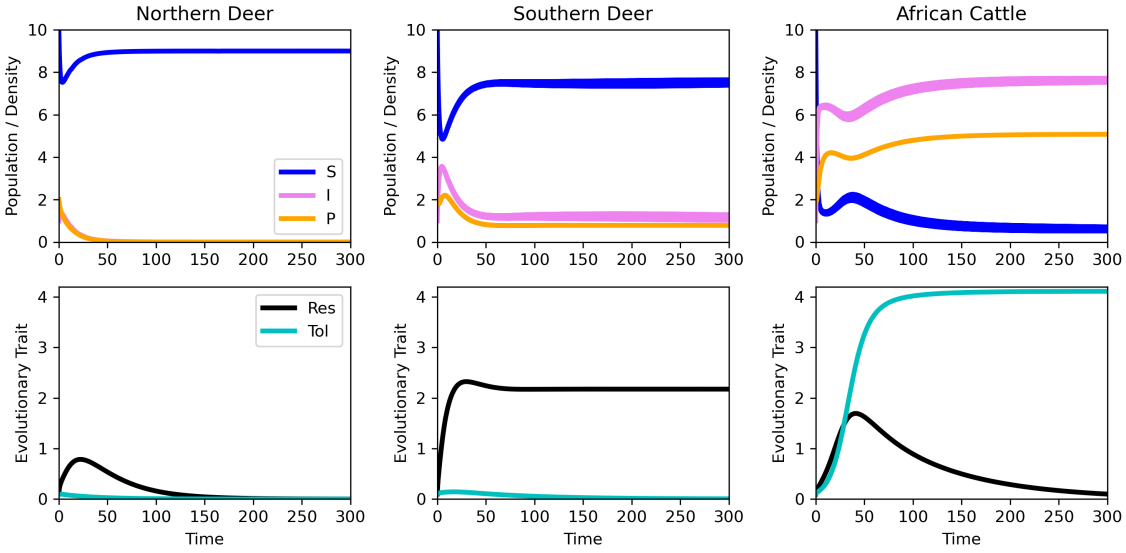

Figure 14. Seasonal dynamics of northern deer, southern deer, and African cattle. Northern deer evolve neither resistance nor tolerance due to low encounter rates with EHDV. Southern deer that are exposed to moderate levels of the pathogen seasonally evolve resistance. African cattle that experience EHDV endemically evolve tolerance.

Our findings are supported empirically. Studies from the Appalachian and Great Plains regions show that northern white-tailed deer populations remain largely immunologically naïve before epizootics and continue to suffer substantial mortality from EHDV outbreaks. Furthermore, there is no evidence of attenuation or improved outcomes over the last four decades [30, 31]. Thus, the (albeit limited) empirical evidence suggests that northern white-tailed deer populations have likely not evolved defense mechanisms against EHD. This matches our model predictions that low, rare exposure to EHDV does not lead to the evolution of resistance or tolerance.

Southern white-tailed deer experience repeated exposure to EHDV year after year, with a predominance of locally circulating serotypes, such as EHDV-2 [32, 33]. Experimental cross-protection studies show that the neutralizing responses to EHDV are largely serotype-specific (antibodies against EHDV-2 did not confer cross-protection against EHDV-1 infection [34]). Maternal antibody transfer is present in these enzootic systems [35]: maternal-antibody-positive fawns are much less likely to become infected but, if infected, present with transient, low-level viremia [36]. This reduction in infection probability and viral loads over time that arise after repeated, homologous exposure is characteristic of a resistance-dominated immune response. This matches our model predictions that moderate, seasonal exposure to EHDV leads to the evolution of a resistance defense mechanism.

In cattle, experimental inoculation with EHDV resulted in prolonged viremia with minimal clinical disease, consistent with tolerance rather than resistance [37, 38]. Since viral loads remained high throughout the studies but the cattle displayed no detectable clinical disease, gross lesions, or clinicopathologic abnormalities, the cattle's adaptive response likely involves mitigating the effects of EHDV rather than clearing the pathogen. This matches our model predictions that high, endemic levels of EHDV promote the evolution of tolerance.

3.4. Impact of control strategies on evolution of defense mechanisms

To study the effect of control mechanisms, we extend our model by considering the dynamics of the biting midge vector. We assume that the midge population M grows logistically with growth rate r_M and carrying capacity K_M and the transmission rate β is proportional to $\frac{M}{K_M}$. We incorporate the control in the vector equation by considering an additional death rate $c \geq 0$ so that $M' = r_M M\left(1 - \frac{M}{K_M}\right) - cM$. To adequately model the midges population, we assume that the growth rate r_M and the carrying capacity K_M are periodic, replicating the increased reproductive strength and resource availability in the summer season, respectively [39, 40]. That is, we consider $r_M(t) = \overline{r}_M + s(t)$ and $K_M(t) = \overline{K}_M + \frac{\overline{K}_M}{2} s(t)$, where $s(t)$ is the functional form introduced in Section 3.3, modeling the increase during the summer season. More precisely, the extended model is

$$
\begin{aligned}
\frac{dS}{dt} &= r(v_r, v_t)(S + I)\left(1 - \gamma(S + I)\right) - \mu S - \overline{\beta}\frac{M}{\overline{K}_M + \frac{\overline{K}_M}{2} s(t)} S P + \phi(v_r) I \\
\frac{dI}{dt} &= \overline{\beta}\frac{M}{\overline{K}_M + \frac{\overline{K}_M}{2} s(t)} S P - \mu I - \alpha(v_t) I - \phi(v_r) I \\
\frac{dP}{dt} &= \omega I - \mu_p P \\
\frac{dv_i}{dt} &= k\left(\frac{\partial}{\partial v_i}\rho(A(v_r, v_t))\right) \\
\frac{dM}{dt} &= (\overline{r}_M + s(t))\, M\left(1 - \frac{M}{\overline{K}_M + \frac{\overline{K}_M}{2} s(t)}\right) - cM
\end{aligned}
$$

where A is projection matrix given in (2.8) and all parameters are being considered positive.

We are interested in whether, and to what extent, different control strategies can have different impacts on the evolution of the defense strategies. To that regard, we consider two controls: a

continuously applied control of strength c and a periodically applied control during the summer season (peak midge activity) of strength $\frac{c}{\ell}$ ($\ell \in (0,1)$ is the length of the summer season). The adjustment of the control strength is intended to make both strategies comparable by equating the mean control intensity over one period. The control is therefore determined by the intensity of the control (c), as well as the seasonal parameters (length of the summer season ℓ and height of the summer season h) in the case of the periodic control. Varying these three control parameters, simulations are run with all other parameter values given in Table 1, unless stated specifically, and with vector specific model parameters $r_M = 3, K_M = 100$.

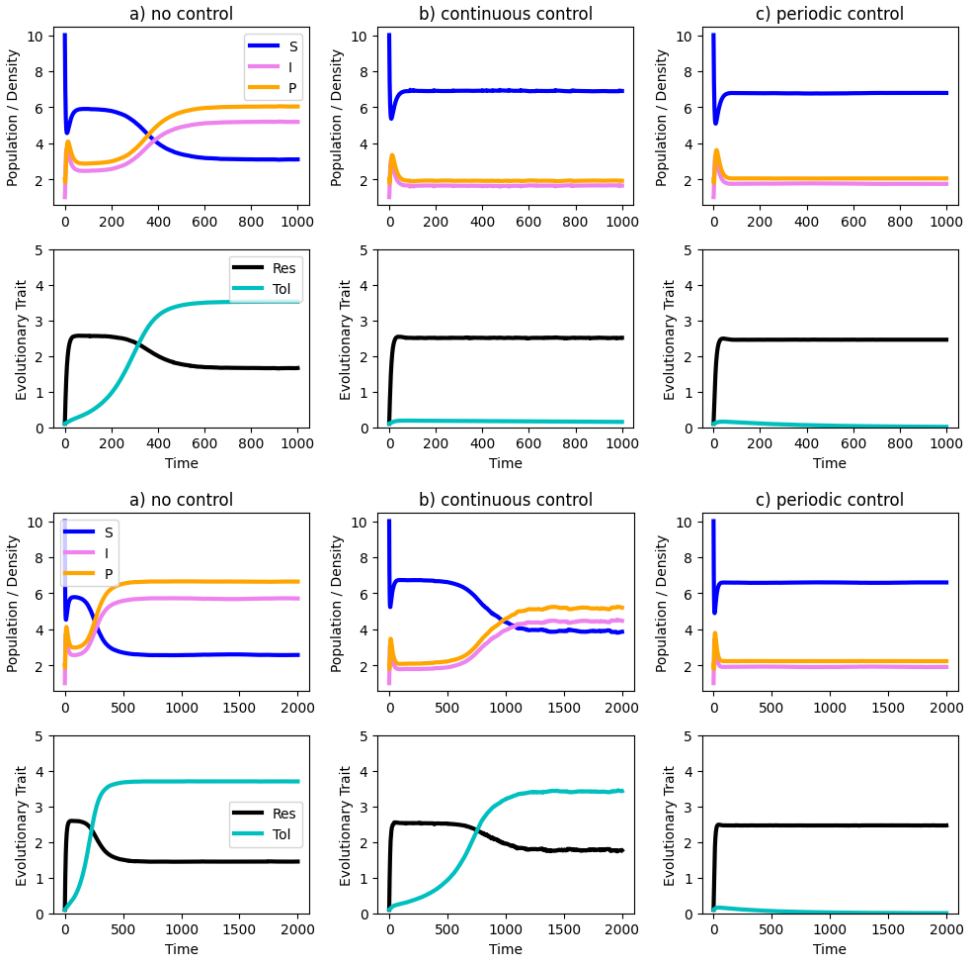

Figure 15. Impact of transmission season length on the evolution of defense mechanisms for moderate seasonal severity and control intensity. Length of the summer season is 20% (30%) in top (bottom) rows. a) No control is applied. b) The death rate is reduced by the rate c continuously. c) The death rate is reduced by $\frac{c}{\ell}$ during the summer season, where $\ell \in (0,1)$ represents the length of the summer season.

First, we investigate the impact of control window duration on the evolution of defense mechanisms. Under moderate seasonal severity and control intensity ($h = 1$ and $c = 0.5$), increasing the length of the transmission season from 20% to 30% of the year changes the favored defense mechanism under continuous control from resistance to tolerance, but not under periodic or no

control, which evolve resistance and tolerance under both seasonal lengths, respectively (Figure 15). This is because shorter transmission seasons concentrate vector reproduction into brief periods that can be effectively suppressed during the remainder of the year, keeping pathogen levels low and favoring resistance. However, broader transmission seasons are associated with longer midge reproduction that can overwhelm the fixed control rate, leading to an outgrowth of the viral population. This increase in pathogen burden coincides with the switch to a tolerance defense mechanism. Since periodic control automatically concentrates efforts within the transmission season, it is more robust to changes in seasonal length. The temporal synchronization between periodic control and seasonality allows effective suppression of pathogen burden and promotes resistance over tolerance in both cases.

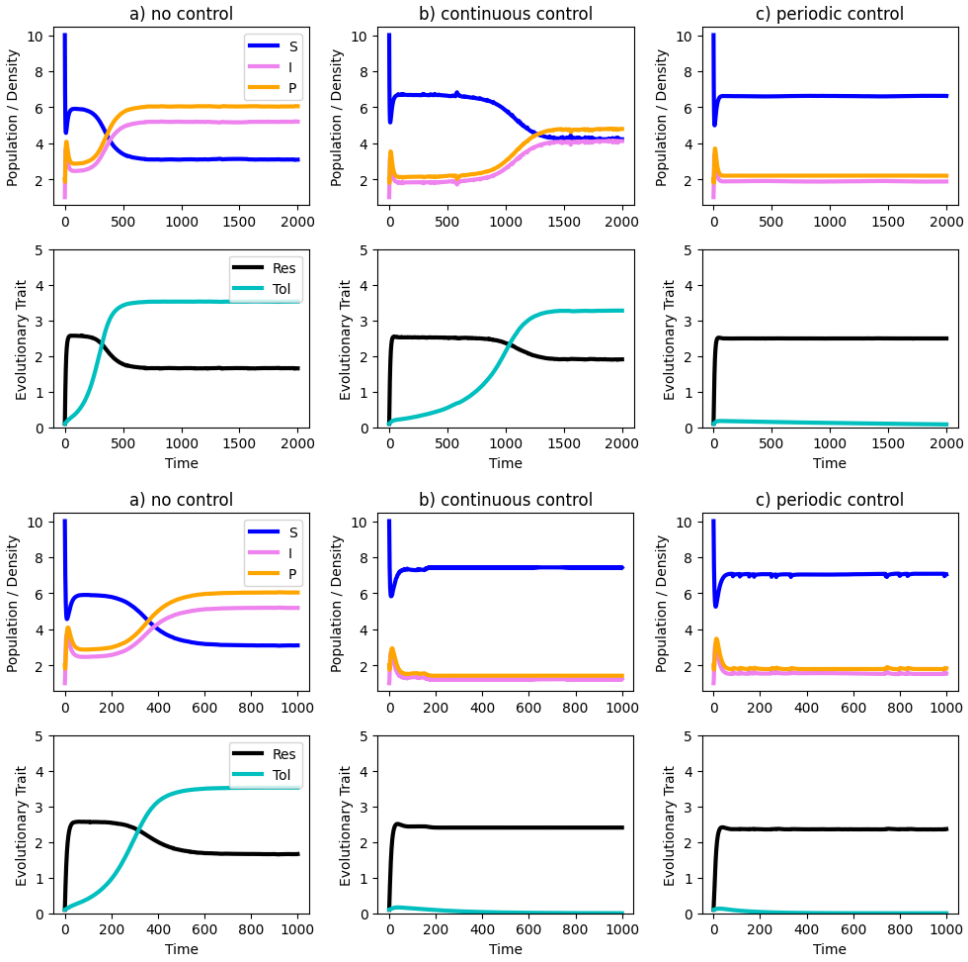

Figure 16. Impact of control intensity on the evolution of defense mechanisms for moderate seasonal severity and short seasonal length. The control intensity increases from moderate levels (top rows) to high values (bottom rows). a) No control is applied. b) The death rate is reduced by the rate c continuously. c) The death rate is reduced by $\frac{c}{\ell}$ during the summer season, where $\ell \in (0, 1)$ represents the length of the summer season.

Next, we explored the impact of control intensity on defense mechanisms. Using moderate seasonal severity ($h = 1$) and setting the seasonal length to $\ell = 0.2$, we find that periodic (no) control

again favors resistance (tolerance) under moderate ($c = 0.4$) and high ($c = 0.7$) control intensities, whereas continuous control promotes tolerance and resistance under moderate and high intensities, respectively (Figure 16). This intensity-dependent variation in defense mechanisms stresses the importance of keeping viral loads low across the year. Under $c = 0.4$, the continuous control is ineffective at suppressing pathogen burden. As before, this increase in viral load (orange curve) paves the path for the evolution of tolerance. When control intensity is increased to $c = 0.7$, this continuous control strategy maintains low viral loads; thus, the host shifts to a resistance strategy. As before, the periodic control strategy that focuses efforts during periods of maximal midge reproduction is effective at forcing low viral loads, even for $c = 0.4$, and thus leads to resistance in both cases.

Perhaps counterintuitively, insufficient control windows and intensity can lead to the evolution of tolerance under periodic control, even when continuous control leads to resistance. Under low seasonal intensity ($h = 0.4$) and control intensity ($c = 0.3$), periodic controls lead to tolerance, whereas continuous controls lead to resistance (Figure 17). This is because the extremely brief period of control application in the periodic case ($\ell = 0.1$) is insufficient to suppress the viral population throughout the rest of the year. Namely, the periodic control leads to "boom-bust" cycles wherein the brief intervention causes a rapid decline in viral load, but is followed by extended periods of uncontrolled growth, eventually leading to the evolution of tolerance over resistance. Aided by the lower seasonal intensities, a continuous strategy proves to be sufficient to suppress the pathogen population, maintaining low burdens throughout the year, leading to the evolution of resistance. It's worth noting that if the control intensity is instead maintained at high levels, we recover similar outcomes to Figure 4, in which hosts evolve neither resistance nor tolerance.

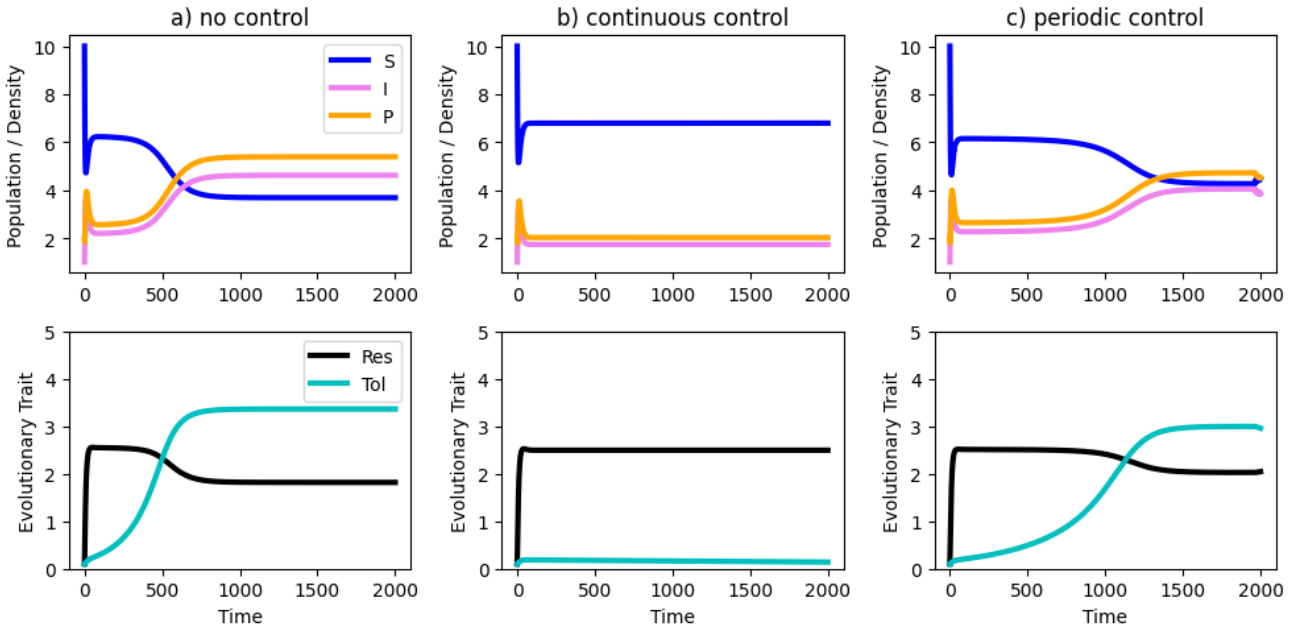

Figure 17. Impact of abbreviated control windows and low control intensity on the evolution of defense mechanisms. a) No control is applied. b) The death rate is reduced by the rate c continuously. c) The death rate is reduced by $\frac{c}{\ell}$ during the summer season, where $\ell \in (0, 1)$ represents the length of the summer season.

4. Conclusions

Understanding the complex eco-evolutionary dynamics of host-pathogen systems is not only useful for basic science, but also for their far-reaching practical implications, ranging from wildlife health to livestock productivity. For example, a severe decline in the deer population due to EHDV across the United States [31, 41, 42] impacts hunting regulations, which is a billion-dollar industry [43], and consequently impacts the economic sector in many regions. Another example is white-nose syndrome in bats, which has led to dramatic population decline and raised concerns about increased crop damage due to the presence of fewer insect-eating bats [44–46]. Similarly, foot-and-mouth disease in cattle and avian influenza in poultry compromise food production and generate significant economic loss for farmers [47–51]. Understanding how hosts develop defense mechanisms against such pathogens and the impact of environmental conditions on this evolution is critical for designing effective interventions.

Hosts can cope with pathogenic selection pressures by evolving resistance (directly reducing pathogen burden) or tolerance (mitigating the negative effects of infection) [4]. Both of these mechanisms come with a physiological cost, and the relative benefit of each strategy depends on the properties of the host, pathogen, and environment. In this paper, we developed a Darwinian epizootic model to show that high pathogen loads, induced by high pathogen shedding rates, high pathogen transmission rates, or low pathogen mortality rates induce an evolution of tolerance. Similarly, high host growth rates (or conversely, low host death rates and low density-dependent growth suppression) favor the evolution of tolerance. Tolerance can be understood as a strategy that allows hosts to persist in the face of severe and recurring pathogen exposure, whereas resistance provides a way to recover rapidly from pathogenic infection; an effective strategy when host exposure to pathogens is lower.

We then considered a specific host-pathogen system of timely importance: EHD. We showed that empirical trends that observe 1) high mortality and low defense mechanisms in northern white-tailed deer, 2) lower mortality and resistance mechanisms in southern white-tailed deer, and 3) subclinical symptoms and tolerance mechanisms in African cattle are consistent with differences in EHDV seasonality. Namely, northern deer that experience cooler temperatures and shorter summers do not experience sufficient selection pressures to evolve resistance or tolerance. Southern deer that experience seasonal outbreaks evolve resistance, allowing them to recover from the virus and re-establish baseline survival levels. African cattle that experience the virus year-round tend to evolve tolerance, as reinfection with EHDV after recovery is likely. We also considered the impact of continuous and periodic control mechanisms on the biting midge population, finding that the type and intensity of the control as well as the length of the transmission season can lead to the evolution of different defense mechanisms in the host population. These findings have implications for the management of wild and domestic ruminant populations, particularly with the introduction of novel EHDV serotypes that tolerant populations may be more readily able to cope with [52]. It is critical to note that our simulation results here are only intended to make predictions on which defense strategies are favored under different environmental circumstances, host properties, and pathogen properties, not to predict the precise temporal trajectory of evolution. In other words, the value of our modeling results lie in their comparative predictions and mechanistic insight. The actual timescale for reaching these evolutionary outcomes in natural populations would depend on factors we do not explicitly consider here, including the genetic architecture of defense traits, effective population size, mutation rates, and the strength of selection. Although our results are qualitatively in accordance with

empirical studies, in future work, we aim to align these theoretical predictions more closely with experimental and observational work in a variety of host-pathogen systems. This will allow us to understand the time-scales on which defense mechanisms evolve and devise control strategies for conservation and recovery efforts in a changing climate.

We hope that our study, which introduced the incorporation of Darwinian dynamics into epizootic systems, will encourage the broader application of Darwinian modeling of evolutionary processes in epidemiology. Our framework, through thoughtful model construction and numerical simulations, illustrated the potential for developing eco-evolutionary models that predict evolving defense mechanisms observed in nature. Through numerical simulations, we demonstrated how ecological and epidemiological parameters, seasonality, and management strategies influence the evolution of defense mechanisms. Future research could build on this by deriving analytical relationships among these factors to predict conditions under which specific defense mechanisms dominate. More applied extensions of this work may explore alternative representations of seasonality, optimal control strategies using optimization theory, or the inclusion of stochastic elements to better capture environmental variability. With that, we intend this work to contribute to the vastly evolving literature of eco-evolutionary modeling.

Use of AI Tools Declaration

The authors declare they have not used Artificial Intelligence (AI) tools in the creation of this article.

Conflict of interest

Yun Kang is a member of the Editorial Board of Mathematical Biosciences and Engineering and was not involved in the editorial review or the decision to publish this article. The authors declare there is no conflict of interest.

References

1. L. Jimenez-Cabello, S. Utrilla-Trigo, G. Lorenzo, J. Ortego, E. Calvo-Pinilla, Epizootic hemorrhagic disease virus: Current knowledge and emerging perspectives, *Microorganisms*, **11** (2023), 1339. https://doi.org/10.3390/microorganisms11051339
2. M. G. Ruder, T. J. Lysyk, D. E. Stallknecht, L. D. Foil, D. J. Johnson, C. C. Chase, et al., Transmission and epidemiology of bluetongue and epizootic hemorrhagic disease in north america: Current perspectives, research gaps, and future directions, *Vector-Borne Zoonotic Dis.*, **15** (2015), 348–363. https://doi.org/10.1089/vbz.2014.1703
3. B. Epstein, M. Jones, R. Hamede, S. Hendricks, H. McCallum, E. P. Murchison, et al., Rapid evolutionary response to a transmissible cancer in Tasmanian devils, *Nat. Commun.*, **7** (2016), 12684. https://doi.org/10.1038/ncomms12684
4. L. Raberg, D. Sim, A. F. Read, Disentangling genetic variation for resistance and tolerance to infectious diseases in animals, *Science*, **318** (2007), 812–814. https://doi.org/10.1126/science.1148526

5. M. Boots, A. Best, M. R. Miller, A. White, The role of ecological feedbacks in the evolution of host defence: what does theory tell us? *Philos. Trans. R. Soc. Lond B Biol. Sci.*, **364** (2009), 27–36. https://doi.org/10.1098/rstb.2008.0160
6. R. Medzhitov, D. S. Schneider, M. P. Soares, Disease tolerance as a defense strategy, *Science*, **335** (2012), 936–941. https://doi.org/10.1126/science.1214935
7. S. Gandon, P. Agnew, Y. Michalakis, Coevolution between parasite virulence and host life-history traits, *Am. Nat.*, **160** (2002), 374–388. https://doi.org/10.1086/341525
8. A. K. Gibson, C. R. Amoroso, Evolution and ecology of parasite avoidance, *Annu. Rev. Ecol. Evol. Syst.*, **53** (2022), 47–67. https://doi.org/10.1146/annurev-ecolsys-102220-020636
9. E. I. Svensson, L. Raberg, Resistance and tolerance in animal enemy-victim coevolution, *Trends Ecol. Evol.*, **25** (2010), 267–274. https://doi.org/10.1016/j.tree.2009.12.005
10. B. C. Sheldon, S. Verhulst, Ecological immunology: Costly parasite defences and trade-offs in evolutionary ecology, *Trends Ecol. Evol.*, **11** (1996), 317–321. https://doi.org/10.1016/0169-5347(96)10039-2
11. A. Bukkuri, J. S. Brown, Evolutionary game theory: Darwinian dynamics and the G function approach, *Games*, **12** (2021), 72. https://doi.org/10.3390/g12040072
12. T. L. Vincent, J. S. Brown, *Evolutionary Game Theory, Natural Selection, and Darwinian Dynamics*, Cambridge University Press, 2009. https://doi.org/10.1017/CBO9780511542633
13. A. Bukkuri, J. S. Brown, Integrating eco-evolutionary dynamics into matrix population models for structured populations: Discrete and continuous frameworks, *Methods Ecol. Evol.*, **14** (2023), 1475–1488. https://doi.org/10.1111/2041-210X.14111
14. R. M. Anderson, R. M. May, The population dynamics of microparasites and their invertebrate hosts, *Philos. Trans. R. Soc. Lond. B Biol. Sci.*, **291** (1981), 451–524. https://doi.org/10.1098/rstb.1981.0005
15. M. Kleshnina, S. Streipert, J. S. Brown, K. Staňková, Game theory for managing evolving systems: Challenges and opportunities of including vector-valued strategies and life-history traits, *Dyn. Games Appl.*, **13** (2023), 1130–1155. https://doi.org/10.1007/s13235-023-00544-5
16. J. M. Cushing, A Darwinian version of the Leslie logistic model for age-structured populations, *Math. Biosci. Eng.*, **22** (2025), 1263–1279. https://doi.org/10.3934/mbe.2025047
17. A. Bukkuri, Modeling stress-induced responses: plasticity in continuous state space and gradual clonal evolution, *Theory Biosci.*, **143** (2024), 63–77. https://doi.org/10.1007/s12064-023-00410-3
18. A. Bukkuri, F. R. Adler, Biomarkers or biotargets? Using competition to lure cancer cells into evolutionary traps, *Evol. Med. Public Health*, **11** (2023), 264–276. https://doi.org/10.1093/emph/eoad017
19. A. Bukkuri, R. A. Gatenby, J. S. Brown, GLUT1 Production in Cancer Cells: A tragedy of the Commons, *npj Syst. Biol. Appl.*, **8** (2022), 22. https://doi.org/10.1038/s41540-022-00229-6
20. A. Bukkuri, K. J. Pienta, I. Hockett, R. H. Austin, E. U. Hammarlund, S. R. Amend, et al., Modeling cancer's ecological and evolutionary dynamics, *Med. Oncol.*, **40** (2023), 109. https://doi.org/10.1007/s12032-023-01968-0

21. J. J. Cunningham, A. Bukkuri, J. S. Brown, R. J. Gatenby, R. A. Gatenby, Coupled source-sink habitats produce spatial and temporal variation of cancer cell molecular properties as an alternative to branched clonal evolution and stem cell paradigms, *Front. Ecol. Evol.*, **9** (2021), 676071. https://doi.org/10.3389/FEVO.2021.676071

22. J. M. Cushing, J. Park, A. Farrell, N. Chitnis, Treatment outcome in an SI model with evolutionary resistance: A Darwinian model for the evolution of resistance, *J. Biol. Dyn.*, **17** (2023), 2255061. https://doi.org/10.1080/17513758.2023.2255061

23. A. Bukkuri, K. J. Pienta, R. H. Austin, E. U. Hammarlund, S. R. Amend, J. S. Brown, A life history model of the ecological and evolutionary dynamics of polyaneuploid cancer cells, *Sci. Rep.*, **12** (2022), 13713. https://doi.org/10.1038/s41598-022-18137-4

24. J. M. Cushing, S. M. Stump, Darwinian dynamics of a juvenile-adult model, *Math. Biosci. Eng.*, **10** (2013), 1017–1044. https://doi.org/10.3934/mbe.2013.10.1017

25. O. Diekmann, J. A. P. Heesterbeek, M. G. Roberts, The construction of next-generation matrices for compartmental epidemic models, *J. R. Soc. Interface*, **7** (2010), 873–885. https://doi.org/10.1098/rsif.2009.0386

26. C. T. Deressa, Y. O. Mussa, G. F. Duressa, Optimal control and sensitivity analysis for transmission dynamics of Coronavirus, *Results Phys.*, **19** (2020), 103642. https://doi.org/10.1016/j.rinp.2020.103642

27. H. S. Rodrigues, M. T. T. Monteiro, D. F. M. Torres, Sensitivity analysis in a dengue epidemiological model, *Conf. Pap. Math.*, **2013** (2013), 721406. https://doi.org/10.1155/2013/721406

28. J. Wu, R. Dhingra, M. Gambhir, J. V. Remais, Sensitivity analysis of infectious disease models: Methods, advances and their application, *J. R. Soc. Interface*, **10** (2013), 20121018. https://doi.org/10.1098/rsif.2012.1018

29. A. Bukkuri, Eco-evolutionary dynamics of structured populations in periodically fluctuating environments: A G function approach, *Theory Biosci.*, **143** (2024), 293–299. https://doi.org/10.1007/s12064-024-00424-5

30. J. K. Gaydos, J. M. Crum, W. R. Davidson, S. S. Cross, S. F. Owen, D. E. Stallknecht, Epizootiology of an epizootic hemorrhagic disease outbreak in west virginia, *J. Wildl. Dis.*, **40** (2004), 383–393. https://doi.org/10.7589/0090-3558-40.3.383

31. E. K. Kring, D. E. Stallknecht, G. J. D'Angelo, M. T. Kohl, C. Bahnson, C. A. Cleveland, et al., Patterns of Hemorrhagic disease in white-tailed deer (Odocoileus Virginianus) in the great plains of the USA, 1982–2020, *J. Wildl. Dis.*, **60** (2024), 670–682. https://doi.org/10.7589/JWD-D-23-00021

32. M. Becker, G. Gentry, C. Husseneder, L. Foil, Seven-year prospective study on yearly incidence of Orbivirus infection of captive white-tailed deer and potential Culicoides vectors, *J. Med. Entomol.*, **61** (2024), 465–472. https://doi.org/10.1093/jme/tjae006

33. D. E. Stallknecht, M. P. Luttrell, K. E. Smith, V. F. Nettles, Hemorrhagic disease in white-tailed deer in texas: A case for enzootic stability, *J. Wildl. Dis.*, **32** (1996), 695–700. https://doi.org/10.7589/0090-3558-32.4.695

34. J. K. Gaydos, W. R. Davidson, F. Elvinger, E. W. Howerth, M. Murphy, D. E. Stallknecht, Cross-protection between epizootic hemorrhagic disease virus serotypes 1 and 2 in white-tailed deer, *J. Wildl. Dis.*, **38** (2002), 720–728. https://doi.org/10.7589/0090-3558-38.4.720

35. J. K. Gaydos, D. E. Stallknecht, D. Kavanaugh, R. J. Olson, E. R. Fuchs, Dynamics of maternal antibodies to hemorrhagic disease viruses (reoviridae: orbivirus) in white-tailed deer, *J. Wildl. Dis.*, **38** (2002), 253–257. https://doi.org/10.7589/0090-3558-38.2.253

36. N. K. Stilwell, L. L. Clarke, E. W. Howerth, C. Kienzle-Dean, A. Fojtik, L. P. Hollander, et al., The effect of maternal antibodies on clinical response to infection with epizootic hemorrhagic disease virus in white-tailed deer (odocoileus virginianus) fawns, *J. Wildl. Dis.*, **57** (2020), 189–193. https://doi.org/10.7589/JWD-D-20-00001

37. M. J. Abdy, E. E. Howerth, D. E. Stallknecht, Experimental infection of calves with epizootic hemorrhagic disease virus, *Am. J. Vet. Res.*, **60** (1999), 621–626. https://doi.org/10.2460/ajvr.1999.60.05.621

38. C. A. Batten, L. Edwards, A. Bin-Tarif, M. R. Henstock, C. A. L. Oura, Infection kinetics of Epizootic Haemorrhagic disease virus serotype 6 in Holstein-Friesian cattle, *Vet. Microbiol.*, **154** (2011), 23–28. https://doi.org/10.1016/j.vetmic.2011.06.018

39. A. C. Gerry, B. A. Mullens, Seasonal abundance and survivorship of Culicoides sonorensis (Diptera: Ceratopogonidae) at a Southern California dairy, with reference to potential bluetongue virus transmission and persistence, *J. Med. Entomol.*, **37** (2000), 675–688. https://doi.org/10.1603/0022-2585-37.5.675

40. X. Zhang, J. Li, A. C. Gerry, Seasonal change and influence of environmental variables on host-seeking activity of the biting midge Culicoides sonorensis at a southern California dairy, USA, *Parasit. Vectors*, **17** (2024), 212. https://doi.org/10.1186/s13071-024-06290-w

41. S. J. Dorak, C. Varga, M. G. Ruder, P. Gronemeyer, N. A. Rivera, D. R. Dufford, et al., Spatial epidemiology of hemorrhagic disease in Illinois wild white-tailed deer, *Sci. Rep.*, **12** (2022), 6888. https://doi.org/10.1038/s41598-022-10694-y

42. D. E. Stallknecht, A. B. Allison, A. W. Park, J. E. Phillips, V. H. Goekjian, V. F. Nettles, et al., Apparent increase of reported hemorrhagic disease in the midwestern and northeastern USA, *J. Wildl. Dis.*, **51** (2015), 348–361. https://doi.org/10.7589/2013-12-330

43. Association of Fish and Wildlife Agencies, Hunting in America: An economic force in conservation, Available from: https://www.fishwildlife.org/application/files/3815/3719/7536/Southwick_Assoc_-_NSSF_Hunting_Econ.pdf.

44. J. R. Hoyt, A. M. Kilpatrick, K. E. Langwig, Ecology and impacts of white-nose syndrome on bats, *Nat. Rev. Microbiol.*, **19** (2021), 196–201. https://doi.org/10.1038/s41579-020-00493-5

45. M. Isidoro-Ayza, J. M. Lorch, B. S. Klein, The skin I live in: Pathogenesis of white-nose syndrome of bats, *PLOS Pathog.*, **20** (2024), 1012342. https://doi.org/10.1371/journal.ppat.1012342

46. S. Perea, E. A. Ferrall, K. M. Morris, P. E. Pattavina, N. Sharp, S. B. Castleberry, A decade of hibernating bat communities along the periphery of a region of white-nose syndrome, *J. Wildl. Manage.*, **88** (2024), 22506. https://doi.org/10.1002/jwmg.22506

47. R. Alders, J. A. Awuni, B. Bagnol, P. Farrell, N. De Haan, Impact of avian influenza on village poultry production globally, *EcoHealth*, **11** (2014), 63–72. https://doi.org/10.1007/s10393-013-0867-x

48. M. F. Boni, A. P. Galvani, A. L. Wickelgren, A. Malani, Economic epidemiology of avian influenza on smallholder poultry farms, *Theor. Popul. Biol.*, **90** (2013), 135–144. https://doi.org/10.1016/j.tpb.2013.10.001

49. I. Capua, S. Marangon, Control of avian influenza in poultry, *Emerging Infect. Dis.*, **12** (2006), 1319–1324. https://doi.org/10.3201/eid1209.060430

50. W. T. Jemberu, M. C. M. Mourits, T. Woldehanna, H. Hogeveen, Economic impact of foot and mouth disease outbreaks on smallholder farmers in Ethiopia, *Prev. Vet. Med.*, **116** (2014), 26–36. https://doi.org/10.1016/j.prevetmed.2014.06.004

51. T. J. D. Knight-Jones, J. Rushton, The economic impacts of foot and mouth disease -What are they, how big are they and where do they occur? *Prev. Vet. Med.*, **112** (2013), 161–173. https://doi.org/10.1016/j.prevetmed.2013.07.013

52. J. K. Gaydos, W. R. Davidson, F. Elvinger, D. G. Mead, E. W. Howerth, D. E. Stallknecht, Innate resistance to epizootic hemorrhagic disease in white-tailed deer, *J. Wildl. Dis.*, **38** (2002), 713–719. https://doi.org/10.7589/0090-3558-38.4.713

Appendix

Calculation of partial derivatives for model (2.9)*:*

We make the following observations

$$\frac{\partial r(v_r,v_t)}{\partial v_r}=\frac{-2v_r}{\sigma_r^2}r(v_r,v_t), \qquad \frac{\partial r(v_r,v_t)}{\partial v_t}=\frac{-2v_t}{\sigma_r^2}r(v_r,v_t)$$

$$\frac{\partial \alpha(v_t)}{\partial v_t}=\frac{-2v_t}{\sigma_\alpha^2}\alpha(v_t), \qquad \frac{\partial \phi(v_r)}{\partial v_r}=\frac{2v_r}{\sigma_\phi^2}\overline{\phi}e^{-\frac{v_r^2}{\sigma_\phi^2}}$$

We also need the following partial derivatives:

$$\frac{\partial \mathrm{tr}(A)}{\partial v_r}=(1-\gamma(S+I))\frac{\partial}{\partial v_r}r(v_r,v_t)-\phi'(v_r)=\frac{-2v_r}{\sigma_r^2}(1-\gamma(S+I))\,r(v_r,v_t)-\frac{2v_r}{\sigma_\phi^2}\overline{\phi}e^{-\frac{v_r^2}{\sigma_\phi^2}} \tag{A.1}$$

$$\frac{\partial \mathrm{tr}(A)}{\partial v_t}=(1-\gamma(S+I))\frac{\partial}{\partial v_t}r(v_r,v_t)-\alpha'(v_t)=\frac{-2v_t}{\sigma_r^2}(1-\gamma(S+I))\,r(v_r,v_t)+\frac{2v_t}{\sigma_\alpha^2}\alpha(v_t) \tag{A.2}$$

Thus, $\frac{\partial}{\partial v_r}\mathrm{tr}(A)=v_rF_r(v_r,v_t)$ for $F_r(v_r,v_t):=-\frac{2}{\sigma_r^2}(1-\gamma(S+I))r(v_r,v_t)-\frac{2}{\sigma_\phi^2}\overline{\phi}e^{-\frac{v_r^2}{\sigma_\phi^2}}$ and $\frac{\partial}{\partial v_t}F_t(v_r,v_t)$ for $F_t(v_r,v_t):=\frac{-2}{\sigma_r^2}(1-\gamma(S+I))\,r(v_r,v_t)+\frac{2}{\sigma_\alpha^2}\alpha(v_t)$. Furthermore,

$$\frac{\partial \det(A)}{\partial v_r}=\frac{\partial}{\partial v_r}\{-r(v_r,v_t)(1-\gamma(S+I))(\mu+\alpha(v_t)+\phi(v_r)+\beta P)+\mu(\mu+\alpha(v_t)+\phi(v_r))+\beta P(\mu+\alpha(v_t))\}$$

$$= \left(\frac{2v_r r(v_r,v_t)}{\sigma_r^2}\right)(1-\gamma(S+I))\,(\mu+\alpha(v_t)+\phi(v_r)+\beta P) - r(v_r,v_t)\,(1-\gamma(S+I))\,\overline{\phi}e^{-\frac{v_r^2}{\sigma_\phi^2}}\frac{2v_r}{\sigma_\phi^2} + \mu\overline{\phi}e^{-\frac{v_r^2}{\sigma_\phi^2}}\frac{2v_r}{\sigma_\phi^2}. \quad \text{(A.3)}$$

Thus, $\frac{\partial}{\partial v_r}\det(A) = v_r G_r(v_r, v_t)$, where

$$G_r(v_r,v_t) = \left(\frac{2r(v_r,v_t)}{\sigma_r^2}\right)(1-\gamma(S+I))\,(\mu+\alpha(v_t)+\phi(v_r)+\beta P) - r(v_r,v_t)\,(1-\gamma(S+I))\,\overline{\phi}e^{-\frac{v_r^2}{\sigma_\phi^2}}\frac{2}{\sigma_\phi^2} + \mu\overline{\phi}e^{-\frac{v_r^2}{\sigma_\phi^2}}\frac{2}{\sigma_\phi^2}.$$

Also

$$\begin{aligned}\frac{\partial}{\partial v_t}\det(A) &= \frac{\partial}{\partial v_t}\{-r(v_r,v_t)\,(1-\gamma(S+I))\,(\mu+\alpha(v_t)+\phi(v_r)+\beta P)+\mu(\mu+\alpha(v_t)+\phi(v_r))+\beta P(\mu+\alpha(v_t))\}\\ &= \left(\frac{2v_t r(v_r,v_t)}{\sigma_r^2}\right)(1-\gamma(S+I))\,(\mu+\alpha(v_t)+\phi(v_r)+\beta P) + r(v_r,v_t)\,(1-\gamma(S+I))\,\alpha(v_t)\frac{2v_t}{\sigma_\alpha^2} - \mu\alpha(v_t)\frac{2v_t}{\sigma_\alpha^2} - \beta P\alpha(v_t)\frac{2v_t}{\sigma_\alpha^2}, \quad \text{(A.4)}\end{aligned}$$

so that $\frac{\partial}{\partial v_t}\det(A) = v_t G_t(v_r, v_t)$ for

$$G_t(v_r,v_t) = \left(\frac{2r(v_r,v_t)}{\sigma_r^2}\right)(1-\gamma(S+I))\,(\mu+\alpha(v_t)+\phi(v_r)+\beta P) + r(v_r,v_t)\,(1-\gamma(S+I))\,\alpha(v_t)\frac{2}{\sigma_\alpha^2} - \mu\alpha(v_t)\frac{2}{\sigma_\alpha^2} - \beta P\alpha(v_t)\frac{2}{\sigma_\alpha^2}.$$

AIMS Press